Asymptotically Good Generalized Quantum Tanner Codes

Olai Å. Mostad, *Student Member, IEEE*, Eirik Rosnes, *Senior Member, IEEE*, and Hsuan-Yin Lin, *Senior Member, IEEE*

***Abstract*—In this work, we present a generalization of the recently proposed quantum Tanner codes by Leverrier and Zémor, which contains a construction of asymptotically good quantum low-density parity-check codes. Quantum Tanner codes have so far been constructed equivalently from groups, Cayley graphs, or square complexes constructed from groups. We show how to enlarge this to graphs with labeled local views and a family of square complexes, which is the largest possible in a certain sense. We show that the proposed generalization contains a family of asymptotically good quantum codes that are based on non-Cayley Schreier graphs, i.e., a *new* family of (generalized) quantum Tanner codes is provided. Moreover, we evaluate the performance of the generalized codes and compare with those based on Cayley graphs both in terms of minimum distance and logical error rate on the depolarizing channel, demonstrating that the proposed generalized codes based on Schreier graphs outperform those based on Cayley graphs.**

***Index Terms*—Asymptotically good quantum low-density parity-check (LDPC) codes, belief propagation decoding, Calderbank-Shor-Steane (CSS) codes, generalized bicycle codes, quantum error correction, quantum Tanner codes, Schreier graphs, square complexes.**

I. Introduction

Quantum computers, which are based on the peculiarities of quantum mechanics, have been predicted to revolutionize several computing tasks for a long time, e.g., solving challenging problems that arise in chemistry and finance. A quantum computer works by taking advantage of the quantum behavior of particles, which makes it possible to have superpositions of states. However, quantum computers are prone to errors due to the fragile nature of quantum states, in particular when the number of states grows. The use of quantum error-correction codes can reduce the effect of such errors and hence make it possible to build large-scale fault-tolerant quantum computers.

The existence of quantum error-correcting codes was first established independently by Shor and Steane in the mid-nineties [2], [3]. Calderbank-Shor-Steane (CSS) codes allowing to build a quantum code from two classical codes with the requirement that the dual of one should be contained in the other [4], [5] were introduced shortly after and then followed by quantum stabilizer codes [6], [7] which are in many ways analogous to classical linear codes. Since then, protecting quantum information has received considerable interest, and it was a long-standing open problem whether asymptotically good quantum low-density parity-check (LDPC) error-correcting codes, i.e., quantum LDPC codes with a minimum distance growing linearly with the block length, could exist. This was largely due to the CSS restriction that made it difficult to directly extend classical asymptotically good code constructions, and was settled in a 2022 paper by Panteleev and Kalachev [8]. Subsequently, the construction in [8] was modified and improved in [9], resulting in a construction with an improved estimate of the minimum distance growth rate. Independently, very similar constructions have also answered a long-standing open question about locally testable classical codes [8], [10]. Before this, in [11], balanced product codes were proposed, and a construction of quantum LDPC codes with a conjectured linear minimum distance growth was outlined. The recent renewed interest in quantum error correction has come due to recent progress in building intermediate-scale quantum computers with 300-1000 qubits, enough to make them close to performing some tasks faster than state-of-the-art classical computers [12]. Moreover, recent work shows that quantum LDPC codes can indeed provide a high error threshold and simultaneously low overhead for fault-tolerant quantum memory [13].

Constructing good finite-length quantum LDPC codes has received significant attention recently (see, e.g., [14]–[16], and references therein), together with enhanced decoding algorithms (see, e.g., [17]–[19], and references therein) as iterative belief propagation (BP) decoding (both binary and nonbinary) in general performs worse than for classical LDPC codes. The degraded performance can usually be explained by a larger number of 4-cycles in the underlying Tanner graphs and a large number of degenerate errors, i.e., correctable errors affecting the logical state equally as different correctable errors. A code is called degenerate if it has degenerate errors, or equivalently, if its minimum distance is higher than the weight of some stabilizer. Topological quantum codes [20]–[27] are an early class of quantum LDPC codes with high noise thresholds and high minimum distance that show poor performance under iterative BP decoding due to high degeneracy.

In this work, we propose a construction of quantum Tanner codes that can loosely be described as follows. Take two regular[1] graphs on the same vertex set. They should satisfy a condition that leads to many 4-cycles in their union. From the

This paper was presented in part at the Quantum Information Knowledge (QuIK) Workshop of the 2024 IEEE International Symposium on Information Theory (ISIT), Athens, Greece, July 2024 [1].

Olai Å. Mostad, E. Rosnes, and H.-Y. Lin are with Simula UiB, N-5006 Bergen, Norway (e-mail: olai@simula.no, eirikrosnes@simula.no, lin@simula.no).

This paper has supplementary material available at http://ieeexplore.ieee.org, provided by the authors. The material includes several technical proofs and an explicit parity-check matrix construction.

[1]A graph is called *regular* if all its vertices have the same degree.

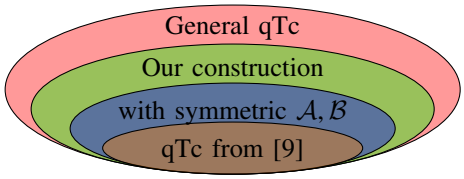

Fig. 1. Our construction (green) generalizes the quantum Tanner codes (qTc) from [9] (brown). We also consider a slightly less general construction (blue), and in Section III-D we show that there are codes not from our construction that also reasonably may be called general quantum Tanner codes (red).

graphs, create a two-dimensional space of squares by filling in certain of these cycles. This type of space is fittingly called a square complex. The two diagonals in a square give rise to two new graphs, and by putting bits on the edges and parity-check constraints at the vertices of these graphs in a clever way, we obtain quantum codes. When applied to bipartite double covers of Cayley graphs, our construction gives the quantum Tanner codes from [9] (see Proposition 4), illustrated by the brown region of Fig. 1.

Theorem 1 gives a necessary and sufficient condition such that if one starts with a graph where this clever assignment is possible, then the graph can always be viewed as the graph of diagonals of a square complex, and this complex can always be made from a pair of graphs. This condition puts us in the green region of Fig. 1. Such an assignment may also be possible without this condition, in which case the resulting codes could still reasonably be called general quantum Tanner codes. Lemma 3 gives a condition for this, putting us in the red region of Fig. 1.

We give several minor results about the pairs of graphs that can be used in our construction and their expansion, culminating in Theorem 2, proving the existence of a family of asymptotically good quantum LDPC codes within our construction and strictly outside the one from [9]. With this, we argue that it may be beneficial to consider our more general approach rather than limiting oneself to left-right Cayley complexes.

Another desirable aspect of quantum Tanner codes is their decoders. Given optimal robustness of local codes, [28] gives an algorithm that corrects errors of linear weight in logarithmic time. Similar decoders are considered in [29] and [30], and also [31] for a closely related construction. These decoders for quantum Tanner codes should be directly applicable to our generalized codes, but we will not consider them here.

Our main contributions are summarized as follows.

- We present a generalization of quantum Tanner codes using more general graphs, which contains the Cayley-based quantum Tanner codes from [9] as a special case. We further show that the proposed generalization contains a family of asymptotically good quantum LDPC codes that are based on non-Cayley Schreier graphs and hence constitute a *new* family of (generalized) quantum Tanner codes, see Theorem 2 for a precise statement. These codes are part of the blue region of Fig. 1, a subset of our codes that are easier to work with (see Section III-B2). In contrast to [1], where only the potential to find other families of asymptotically good codes was argued, we here provide an actual construction.
- In order to assess the proposed generalization, we provide extensive numerical results showing that the generalized codes in several cases can provide better spectral expansion properties as verified through a computer search for selected code lengths and also give a lower logical error rate compared to Tanner codes based on Cayley graphs as demonstrated on the depolarizing channel. These findings are backed by minimum distance calculations, which show that higher minimum distances can be obtained.

Independently, another code construction of quantum LDPC codes from high-dimensional expanders has been studied in [32]. The authors construct quantum locally testable codes from a cubical complex and local codes. In the two-dimensional case, bits are placed on the edges, and checks are placed on both the vertices and the squares, differing from quantum Tanner codes, which have bits on the squares. A certain family of four-dimensional cubical complexes result in codes with constant rate, query complexity, and inverse-polylogarithmic relative minimum distance and soundness. To achieve this, they extend beyond Cayley graphs, as we do here and in our conference version of this work [1]. We view this as further evidence that this generalization is worthwhile. Their labeling sets are assumed to be symmetric, meaning that codes constructed using their complexes with our proposed method would fall within the blue region of Fig. 1, while the graphs we allow for are as general as possible in the sense of Corollary 1.

A. Notation

Vectors are denoted by bold letters, matrices by sans serif uppercase letters, and sets (and groups) by calligraphic uppercase letters, e.g., $\boldsymbol{a}$, A, and $\mathcal{A}$, respectively. The neutral element of a group will be denoted by 1, while e is reserved for an edge in a graph. We denote the group of integers by $\mathcal{Z}$ and the cyclic group on m elements by $\mathcal{Z}_m$. Linear codes, graphs, and square complexes are denoted by script uppercase letters, e.g., $\mathscr{C}$. A graph with vertex set $\mathcal{V}$ and edge set $\mathcal{E}$ is denoted by $\mathscr{G} = (\mathcal{V}, \mathcal{E})$, and may have parallel edges and self-loops unless stated otherwise. The edges incident to a vertex v is called the local view of v and denoted $\mathcal{E}(v)$. We will assume the vertex and edge sets of a graph to be ordered. The notation (v, w) is used for an undirected edge between the vertices v and w. For digraphs, we write $(\overrightarrow{v, w})$ for an edge directed from v to w. The disjoint union of sets $\mathcal{A}, \mathcal{B}$ is denoted by $\mathcal{A} \sqcup \mathcal{B} \triangleq \{(a, 0), (b, 1) : a \in \mathcal{A}, b \in \mathcal{B}\}$. A permutation π of a set $\mathcal{A}$ is sometimes written in standard cycle notation $(x, \pi(x), \pi(\pi(x)), \dots), \dots, (y, \pi(y), \dots)$. A linear code $\mathscr{C}$ of length n, dimension k, and minimum distance d is sometimes referred to by $[n, k, d]$, and its dual code is denoted $\mathscr{C}^\perp$. The binary field is denoted by $\mathbb{F}_2$, the identity matrix of size a by I_a, the all-zero matrix (of arbitrary size) by $\mathsf{0}$, and the transpose of a matrix by $(\cdot)^\intercal$. Hamming weight of vectors and order of sets are denoted by $|\cdot|$. Standard order notation $\Theta(\cdot)$ and $O(\cdot)$ is used for asymptotic results. The natural numbers are denoted by $\mathbb{N}$, and given $n \in \mathbb{N}$, we define $[n] \triangleq \{1, 2, \dots, n\}$. A quantum code with length n and code dimension k is denoted as $[[n, k]]$, or more explicitly as $[[n, k, d]]$ when the minimum distance d is specified.

II. PRELIMINARIES

We recall some background on particular types of graphs, their (spectral) expansion, definitions of classical and quantum error-correcting codes, and the notion of a square complex.

A. Graphs

An undirected graph without self-loops can be viewed as a digraph by replacing edges (v, w) by pairs of directed edges $(\overrightarrow{v,w}), (\overrightarrow{w,v})$, yielding a digraph with twice as many edges as the graph, see Example 1 below. When doing this for graphs with self-loops, one has to specify whether an undirected self-loop corresponds to two undirected self-loops or one. We allow for this choice to be individual for each edge.

Definition 1. *A labeling η on a digraph $(\mathcal{V}, \mathcal{E})$ by elements of $\mathcal{A}$ is a function $\eta : \mathcal{E} \to \mathcal{A}$. A digraph with a labeling is called a labeled digraph, and we say it is well-labeled if for every vertex $v \in \mathcal{V}$ and label $a \in \mathcal{A}$ there is exactly one edge starting at v labeled by a and exactly one edge ending in v labeled by a.*

A labeling on the local views of an undirected graph is equivalent to a labeling on the corresponding digraph. An edge $v \overset{e}{—} w$ corresponds to a pair of directed edges $v \xrightarrow{\vec{e}} w$, $v \xleftarrow{\overleftarrow{e}} w$, and we use the convention that e has the label of $\vec{e}$ in the local view of v and the label of $\overleftarrow{e}$ in the local view of w. We write $s(\vec{e}) = v = t(\overleftarrow{e})$ and $t(\vec{e}) = w = s(\overleftarrow{e})$, where "$s$" and "$t$" indicate the source and target vertices of a directed edge, respectively. For bipartite graphs with vertex set $\mathcal{V} = \mathcal{V}_0 \sqcup \mathcal{V}_1$, we let $\vec{e}$ go from $\mathcal{V}_0$ to $\mathcal{V}_1$. Given a (undirected) graph $(\mathcal{V}, \mathcal{E})$, we write $\mathcal{E}^{\mathrm{dir}}$ for the edges of the corresponding digraph.

We will say that a graph has *labeled local views* if for every vertex $v \in \mathcal{V}$ and label $a \in \mathcal{A}$ there is exactly one edge in the local view of v labeled a in that local view.

Given a group $\mathcal{G}$, we will call a subset $\mathcal{A} \subseteq \mathcal{G}$ *symmetric* if $a^{-1} \in \mathcal{A}$ for all $a \in \mathcal{A}$.

Definition 2. *Given a group $\mathcal{G}$ and a symmetric subset $\mathcal{A} \subseteq \mathcal{G}$, the left Cayley graph $\mathrm{Cay}_{\mathrm{l}}(\mathcal{G}, \mathcal{A})$ is the regular graph with vertex set $\mathcal{G}$ and an edge (g, g') if $g' = ag$ for an $a \in \mathcal{A}$, in which case we label the edge by a and a^{-1} in the local view of g and g', respectively.*[2]

Right Cayley graphs $\mathrm{Cay}_{\mathrm{r}}(\mathcal{G}, \mathcal{A})$ are defined similarly.

Definition 3. *A group action of $\mathcal{G}$ on $\mathcal{V}$ is a function $\varphi : \mathcal{G} \times \mathcal{V} \to \mathcal{V}$ such that $\varphi(1, v) = v$ and $\varphi(g, \varphi(h, v)) = \varphi((gh), v)$ for all $v \in \mathcal{V}$ and $g, h \in \mathcal{G}$, where 1 is the neutral element of $\mathcal{G}$.*

We write gv for $\varphi(g, v)$ to simplify the notation. A group action is called *faithful* when $g = 1$ is the only $g \in \mathcal{G}$ that acts trivially on $\mathcal{V}$, i.e., such that $gv = v$ for all $v \in \mathcal{V}$, *free* when $g = 1$ is the only $g \in \mathcal{G}$ such that $gv = v$ for some $v \in \mathcal{V}$, *transitive* when for any $v, w \in \mathcal{V}$, there is a $g \in \mathcal{G}$ such that $gv = w$, and *regular* when it is free and transitive.

[2]Cayley and Schreier graphs are often defined to have symmetric labeling sets and such that they have no self-loops or parallel edges.

Definition 4. *Given a group $\mathcal{G}$ acting on a set $\mathcal{V}$ and a subset $\mathcal{A} \subseteq \mathcal{G}$, the Schreier digraph defined by $\mathcal{G}$, $\mathcal{V}$, and $\mathcal{A}$ is the digraph with vertices $\mathcal{V}$ and an edge $(\overrightarrow{v,w})$ labeled a whenever there is an $a \in \mathcal{A}$ mapping v to w by the group action. A Schreier graph $\mathrm{Sch}(\mathcal{G}, \mathcal{V}, \mathcal{A})$ is constructed from the Schreier digraph on $\mathcal{G}$, $\mathcal{V}$, and $\mathcal{A}$ by choosing a set of pairs $v \rightleftarrows w$ of edges such that every (directed) edge is part of exactly one pair, and then making an edge (v, w) for each pair on the above form.*[2,3]

For symmetric $\mathcal{A}$, we will pair edges with inverse labels, as we do for Cayley graphs. Note that a directed edge can be paired with itself if it is a self-loop. It is known that all regular graphs can be given the structure of a Schreier graph where $\mathcal{A}$ is not necessarily symmetric.

Example 1. *Let $\mathcal{V} = \{1, 2, 3, 4, 5\}$ and define the permutations $a_1 = (2\ 3\ 5)(1)(4)$, $a_2 = (5\ 3\ 2)(1)(4)$, and $a_3 = (1\ 2)(3\ 4)(5)$. Note that $a_1^{-1} = a_2$ and $a_3^{-1} = a_3$. Next, let $\mathcal{G}$ be the group generated by $\mathcal{A} = \{a_1, a_2, a_3\}$. Then $Sch(\mathcal{G}, \mathcal{V}, \mathcal{A})$ is the following graph, with labeled local views as indicated.*

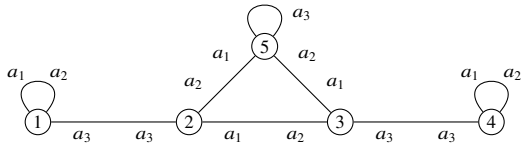

Note that this graph is not regular. Schreier graphs with a symmetric labeling set, like this one, are also often pictured in the following way.

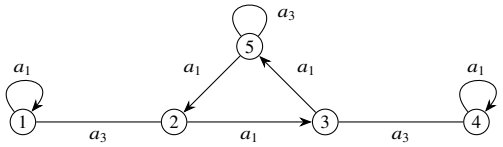

The knowledge that $a_2 = a_1^{-1}$ makes this simpler picture sufficient. Figs. 2 and 3 below follow this convention, where edges without an arrow tip have the same label in both directions. Viewing the graph as a labeled digraph turns out to be useful for us, mainly for notational purposes. The graph then becomes the following regular digraph.

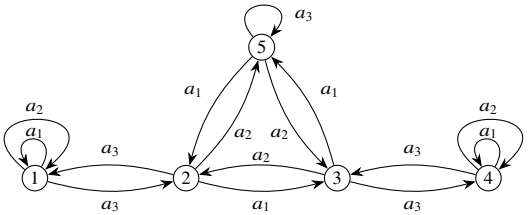

Remark 1. *Schreier graphs are graphs with labeled local views so that the corresponding digraph is well-labeled, and hence also regular. Cayley graphs are the Schreier graphs where the vertex set is the group $\mathcal{G}$ and $\mathcal{A}$ is symmetric, i.e.,*

[3]Not every Schreier digraph can be made into a Schreier graph in this way. A different way to go from digraphs to graphs is by forgetting the direction of each directed edge. We do not use this here, as it would give too many parallel edges (at least in the case where there are self-inverse $a \in \mathcal{A}$).

$\mathrm{Cay}_{\mathrm{l}}(\mathcal{G},\mathcal{A}) = \mathrm{Sch}(\mathcal{G},\mathcal{G},\mathcal{A})$ *when* $\mathcal{G}$ *acts on the left. Both are labeled by the group elements* $\mathcal{A} \subseteq \mathcal{G}$.

By Cayley's theorem [33], the elements of any group can be viewed as permutations of a set, turning the multiplication of elements in the group into a composition of functions. Going the other way, a set of permutations on a set $\mathcal{V}$ will generate a group and define a directed Schreier graph of that group with vertex set $\mathcal{V}$. Concretely, we get a directed edge $v \to w$ labeled π if $\pi(v) = w$.

With a stricter definition of Schreier graphs, most regular graphs are still Schreier.

Proposition 1 ([34])**.** *All regular graphs of even degree can be given the structure of a Schreier graph with a symmetric labeling set. The same is true for graphs of odd degrees precisely when they have a perfect matching.*[4]

We will look at group actions of products of groups, i.e., commuting group actions (see Remark 4), and the following well-known facts will be useful.

Lemma 1. *Two permutations* $\pi_1, \pi_2 : \mathcal{V} \to \mathcal{V}$ *commute if and only if* π_2 *is a digraph homomorphism on the digraph* $\mathscr{G}_1 = (\mathcal{V}, \mathcal{E}_1)$ *where* $\mathcal{E}_1 = \{(\overrightarrow{v, \pi_1(v)}) : v \in \mathcal{V}\}$*, i.e.,* $(\overrightarrow{\pi_2(v), \pi_2(w)}) \in \mathcal{E}_1$ *whenever* $(\overrightarrow{v,w}) \in \mathcal{E}_1$.

Proof: We have $(\overrightarrow{v,w}) \in \mathcal{E}_1$ if and only if $w = \pi_1(v)$, and the permutations π_1 and π_2 commute if and only if $\pi_2(\pi_1(v)) = \pi_1(\pi_2(v))$ for every $v \in \mathcal{V}$, so $(\overrightarrow{\pi_2(v), \pi_2(w)}) \in \mathcal{E}_1$ for every edge $(\overrightarrow{v,w}) \in \mathcal{E}_1$ precisely when the permutations commute. ∎

Proposition 2. *If a group* $\mathcal{G}$ *acts transitively and faithfully on a set* $\mathcal{X}$*, then it acts regularly if and only if* $\mathrm{Aut}_{\mathcal{G}}(\mathcal{X})$ *acts transitively (and hence regularly), where* $\mathrm{Aut}_{\mathcal{G}}(\mathcal{X})$ *is the group of functions* $\sigma : \mathcal{X} \to \mathcal{X}$ *satisfying* $\sigma(gx) = g\sigma(x)$ *for all* $x \in \mathcal{X}, g \in \mathcal{G}$.

We add a proof for completeness.

Proof: Appendix A-A in the supplementary material. ∎

Definition 5. *We say graphs* $\mathscr{G}_{\mathrm{A}} = (\mathcal{V}, \mathcal{E}_{\mathrm{A}})$ *and* $\mathscr{G}_{\mathrm{B}} = (\mathcal{V}, \mathcal{E}_{\mathrm{B}})$ *commute if they come with labeled local views such that the following holds, where* η_{A} *and* η_{B} *are the respective labelings. Any edges* $v_0 \xleftarrow{\vec{e}_1} v_1 \xleftarrow{\vec{e}_2} v_2 \xrightarrow{\vec{e}_3} v_3 \xrightarrow{\vec{e}_4} v_4$ *such that* $e_1, e_3 \in \mathcal{E}_{\mathrm{A}}$*,* $e_2, e_4 \in \mathcal{E}_{\mathrm{B}}$*,* $\eta_{\mathrm{A}}(\vec{e}_1) = \eta_{\mathrm{A}}(\vec{e}_3)$*, and* $\eta_{\mathrm{B}}(\vec{e}_2) = \eta_{\mathrm{B}}(\vec{e}_4)$*, satisfy* $v_0 = v_4$.

We will say the graphs have overlapping edges if there is a pair of vertices v, w *such that both graphs have at least one edge between* v *and* w.

Note that Schreier graphs commute if and only if their defining permutations commute pairwise, hence the name. We generally denote commuting graphs by $\mathscr{G}_{\mathrm{A}}$ and $\mathscr{G}_{\mathrm{B}}$. The notation will also be used for commuting graphs that are input to our main construction, see Definition 10.

[4]A perfect matching is a set of edges where no edges share endpoints and all vertices are endpoints of edges in the set. We allow for self-loops in this set of edges.

B. Graph Expansion

By picking an order on the vertices of a digraph $\mathscr{G} = (\mathcal{V}, \mathcal{E})$, we get an adjacency matrix $\mathsf{M}^{\mathscr{G}}$ where $\mathsf{M}^{\mathscr{G}}_{ij}$ is the number of edges from the j-th vertex to the i-th vertex. We let the adjacency matrix of a graph be the one of the corresponding digraph, uniquely defined when the graph has labeled local views or no self-loops.

Since $\mathsf{M}^{\mathscr{G}}$ is symmetric for any graph $\mathscr{G}$, it will have real eigenvalues $\lambda_1 \geq \cdots \geq \lambda_{|\mathcal{V}|}$, where $\lambda_1 = \Delta$ when the underlying digraph of $\mathscr{G}$ is Δ-regular, and $\lambda_{|\mathcal{V}|} = -\Delta$ if and only if it also is bipartite [35]. For $\mathscr{G}$ connected and $|\mathcal{V}| > 2$, define $\lambda(\mathscr{G}) \triangleq \max\{|\lambda_i| \colon \lambda_i \neq \pm\Delta\}$. When $\mathscr{G}$ has several components (i.e. is disconnected), we set $\lambda(\mathscr{G}) = \Delta$. This is a measure of the (spectral) expansion of the graph, and the graph is called *Ramanujan* when $\lambda(\mathscr{G}) \leq 2\sqrt{\Delta - 1}$ [35].

We now recall a version of the Expander Mixing Lemma, which justifies our interest in graphs with good spectral expansion. Given two sets of vertices $\mathcal{S}$ and $\mathcal{T}$, we let $\mathcal{E}(\mathcal{S}, \mathcal{T})$ denote the set of edges between the two sets.

Lemma 2 (Expander Mixing Lemma [36])**.** *For a* Δ*-regular bipartite, connected graph* $\mathscr{G}$ *with vertex set* $\mathcal{V}_0 \sqcup \mathcal{V}_1$ *and sets* $\mathcal{S} \subseteq \mathcal{V}_0$*,* $\mathcal{T} \subseteq \mathcal{V}_1$*, it holds that*

$$|\mathcal{E}(\mathcal{S}, \mathcal{T})| \leq \frac{\Delta}{|\mathcal{V}_0|}|\mathcal{S}||\mathcal{T}| + \lambda(\mathscr{G})\sqrt{|\mathcal{S}||\mathcal{T}|}.$$

Given a labeling $\eta : \mathcal{E} \to \mathcal{A}$ on a digraph $\mathscr{G} = (\mathcal{V}, \mathcal{E})$, one can write $\mathscr{G}$ as the union of the digraphs $\mathscr{G}^a = \big(\mathcal{V}, \eta^{-1}(\{a\})\big)$ for $a \in \mathcal{A}$. Each of these digraphs has its own adjacency matrix, and these sum to the adjacency matrix of $\mathscr{G}$.

Remark 2. *Given two labeled digraphs* $\mathscr{G}_{\mathrm{A}}, \mathscr{G}_{\mathrm{B}}$ *where the outgoing edges for each vertex have unique labels and the labelings induce* $\mathsf{M}^{\mathscr{G}_{\mathrm{A}}} = \sum_{a \in \mathcal{A}} \mathsf{M}^{\mathscr{G}^a_{\mathrm{A}}}$ *and* $\mathsf{M}^{\mathscr{G}_{\mathrm{B}}} = \sum_{b \in \mathcal{B}} \mathsf{M}^{\mathscr{G}^b_{\mathrm{B}}}$*, they commute if and only if the matrices* $\mathsf{M}^{\mathscr{G}^a_{\mathrm{A}}}$ *and* $\mathsf{M}^{\mathscr{G}^b_{\mathrm{B}}}$ *commute for all* $a \in \mathcal{A}, b \in \mathcal{B}$*. If the labeling sets are also symmetric, then one can add together the adjacency matrices* $\mathsf{M}^{\mathscr{G}^a_{\mathrm{A}}}$ *and* $\mathsf{M}^{\mathscr{G}^{a^{-1}}_{\mathrm{A}}}$ *when* $a \neq a^{-1}$ *and still check commutation of labeled graphs using these matrices. In this case, these matrices will all be symmetric (i.e., equal to their transposed).*

C. Tanner Codes and Quantum CSS Codes

Tanner codes were introduced by Tanner in [37] and famously give asymptotically good families of classical codes. Loosely speaking, the construction takes a graph, puts bits on the edges of the graph, and assigns a code to each vertex. We will be using a regular graph (without self-loops) with the same code on every vertex. A choice of bits is then in the Tanner code if, for any vertex, the bits on the edges connected to the vertex are in the code assigned to it. Formally, we use the following definition, where the restriction of a vector $\boldsymbol{c} \in \mathbb{F}_2^{|\mathcal{E}|}$ defined on the edges $\mathcal{E}$ of a graph to the local view of a vertex v is denoted $\boldsymbol{c}_v$. Note that we assume an ordering on $\mathcal{E}$ so that we may use $\mathbb{F}_2^{|\mathcal{E}|}$ instead of $\{\mathcal{E} \to \mathbb{F}_2\}$ as our vector space.

Definition 6. *Let* $\mathscr{C}$ *be a linear code of length* Δ *and* $\mathscr{G} = (\mathcal{V}, \mathcal{E})$ *be a* Δ*-regular graph, possibly with parallel edges but without self-loops. We define the Tanner code on* $\mathscr{G}$ *and* $\mathscr{C}$ *as* $\mathrm{Tan}(\mathscr{G}, \mathscr{C}) \triangleq \{\boldsymbol{c} \in \mathbb{F}_2^{|\mathcal{E}|} \colon \boldsymbol{c}_v \in \mathscr{C} \text{ for all } v \in \mathcal{V}\}$.

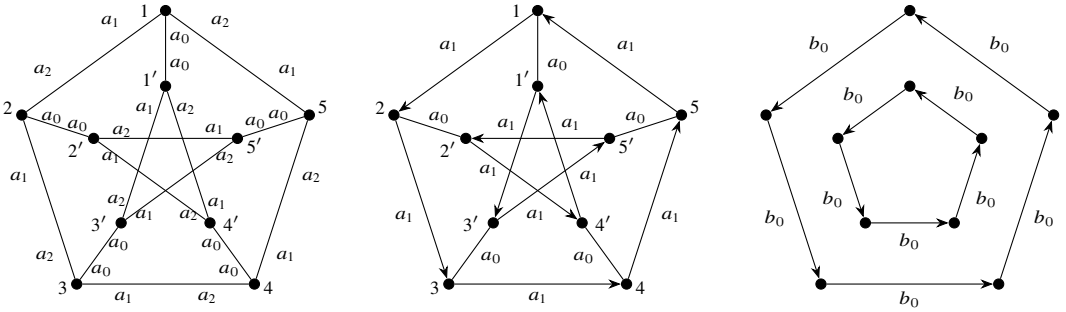

Fig. 2. The Petersen graph is shown to the left. The middle graph is its underlying digraph, with only the labels a_0 and a_1 shown. On the right is a Schreier graph commuting with the Petersen graph, depicted similarly. They are labeled by $\mathcal{A} = \{a_0, a_1, a_2\}$ and $\mathcal{B} = \{b_0, b_1\}$, respectively, where $a_0^{-1} = a_0$, $a_1^{-1} = a_2$, and $b_0^{-1} = b_1$. Note that for the two pictures to the right, the picture together with the inverses uniquely defines the undirected graph, see also Example 1.

The definition assumes that $\mathscr{G}$ has labeled local views. One may think of this as an order on each local view, where each order is independent of the other orderings. More general definitions (for example, Tanner's original one [37]) as well as less general definitions (i.e., the usual Tanner codes of a classical LDPC code) are considered elsewhere. See also the sheaf codes of [38].

For our main construction, the local code $\mathscr{C}$ will be the dual of a tensor product code.

Definition 7. *Given linear codes $\mathscr{C}_\mathrm{A}, \mathscr{C}_\mathrm{B}$ of length n_A and n_B, respectively, their tensor code $\mathscr{C}_\mathrm{A} \otimes \mathscr{C}_\mathrm{B}$ is defined as the set of $n_\mathrm{A} \times n_\mathrm{B}$ matrices with columns in $\mathscr{C}_\mathrm{A}$ and rows in $\mathscr{C}_\mathrm{B}$.*

If $\mathscr{C}_\mathrm{A}$ and $\mathscr{C}_\mathrm{B}$ have parameters $[n_\mathrm{A}, k_\mathrm{A}, d_\mathrm{A}]$ and $[n_\mathrm{B}, k_\mathrm{B}, d_\mathrm{B}]$, respectively, then $\mathscr{C}_\mathrm{A} \otimes \mathscr{C}_\mathrm{B}$ has parameters $[n_\mathrm{A} n_\mathrm{B}, k_\mathrm{A} k_\mathrm{B}, d_\mathrm{A} d_\mathrm{B}]$. The dual code $(\mathscr{C}_\mathrm{A} \otimes \mathscr{C}_\mathrm{B})^\perp$ is equal to $\mathscr{C}_\mathrm{A}^\perp \otimes \mathbb{F}_2^{n_\mathrm{B}} + \mathbb{F}_2^{n_\mathrm{A}} \otimes \mathscr{C}_\mathrm{B}^\perp$ and has minimum distance $\min(d_\mathrm{A}, d_\mathrm{B})$.

Definition 8. *We say the classical codes $\mathscr{C}_0$ and $\mathscr{C}_1$ form a CSS code when $\mathscr{C}_0^\perp \subseteq \mathscr{C}_1$.*

If the classical codes $\mathscr{C}_0$ and $\mathscr{C}_1$ have parity-check matrices H_0 and H_1, respectively, Definition 8 is equivalent to $\mathsf{H}_0 \mathsf{H}_1^\mathsf{T} = 0$. CSS codes were introduced in [4], where they show that the classical codes $\mathscr{C}_0$ and $\mathscr{C}_1$ can be used to construct good quantum error-correcting codes.

The dimension k of a CSS code where the classical codes are of length n is $k = \dim(\mathscr{C}_0 \setminus \mathscr{C}_1^\perp) = \dim \mathscr{C}_0 + \dim \mathscr{C}_1 - n$, and the minimum distance d of the quantum CSS code can be given as the minimum of $d_\mathrm{X} = \min_{\boldsymbol{c} \in \mathscr{C}_0 \setminus \mathscr{C}_1^\perp} |\boldsymbol{c}|$ and $d_\mathrm{Z} = \min_{\boldsymbol{c} \in \mathscr{C}_1 \setminus \mathscr{C}_0^\perp} |\boldsymbol{c}|$.

A CSS code $(\mathscr{C}_0, \mathscr{C}_1)$ is called a *quantum LDPC* code when both codes $\mathscr{C}_0$ and $\mathscr{C}_1$ are defined by sparse parity-check matrices. For families of codes, we require that the columns and rows of the parity-check matrices have weight at most Δ, for some constant Δ independent of the code length n. A code family is called *asymptotically good* if it has parameters $[[n, k = \Theta(n), d = \Theta(n)]]$.

D. Square Complexes

We will need the notion of square complexes, normally defined as two-dimensional cube complexes, a particular type of CW complex [39]. We will use the following definition, which is equivalent for our purposes.

Definition 9. *A square complex $\mathcal{X} = (\mathcal{V}, \mathcal{E}, \mathcal{Q})$ is a triple of sets*[5] *such that $(\mathcal{V}, \mathcal{E})$ is a graph and the elements of $\mathcal{Q}$ are of the form $((v_1, v_2), (v_1, v_3), (v_2, v_4), (v_3, v_4)) \in \mathcal{E}^{\times 4}$.*

III. Proposed Generalized Construction

We start by giving an example of commuting non-Cayley Schreier graphs. Then, we give a construction of quantum LDPC codes that generalize the quantum Tanner codes of [9] and can take these graphs as input. We compare the two constructions and characterize the new one in three different ways.

A. Example

The Petersen graph [40], pictured to the left in Fig. 2, is known to be a non-Cayley graph. It is a Schreier graph, which can be constructed using the group $\mathcal{Z} * \mathcal{Z}_2 \triangleq \{g_1 h_1 \dots g_k h_k : k \in \mathbb{N}, g_i \in \mathcal{Z}, h_i \in \mathcal{Z}_2, \forall i \in [k]\}$ as in Definition 4 [41]. However, it will be more useful for us to view it as two 5-cycles joined in a certain way. Let

$$\mathsf{C}_5 = \begin{bmatrix} 0&1&0&0&1 \\ 1&0&1&0&0 \\ 0&1&0&1&0 \\ 0&0&1&0&1 \\ 1&0&0&1&0 \end{bmatrix} \quad \text{and} \quad \mathsf{C}_5' = \begin{bmatrix} 0&0&1&1&0 \\ 0&0&0&1&1 \\ 1&0&0&0&1 \\ 1&1&0&0&0 \\ 0&1&1&0&0 \end{bmatrix}$$

denote different adjacency matrices for a 5-cycle (vertices labeled by $1, 2, \dots, 5$ for C_5 and vertices labeled by $1', \dots, 5'$ for C_5' in the left graph in Fig. 2). In a certain basis, the Petersen graph has the adjacency matrix

$$\mathsf{M}_\mathrm{A} = \left[\begin{array}{c|c} \mathsf{C}_5 & \mathsf{I}_5 \\ \hline \mathsf{I}_5 & \mathsf{C}_5' \end{array}\right] = \left[\begin{array}{c|c} \mathsf{C}_5 & 0 \\ \hline 0 & \mathsf{C}_5' \end{array}\right] + \left[\begin{array}{c|c} 0 & \mathsf{I}_5 \\ \hline \mathsf{I}_5 & 0 \end{array}\right].$$

Each of these matrices commutes with $\mathsf{M}_\mathrm{B} = \left[\begin{array}{c|c} \mathsf{C}_5 & 0 \\ \hline 0 & \mathsf{C}_5 \end{array}\right]$, the adjacency matrix of the second graph depicted in Fig. 2, so the pair of graphs gives an example of a non-Cayley graph commuting with a 2-component graph when labeled as in the figure, as explained in Remark 2. By reordering the vertices, one can also write the adjacency matrices as $\mathsf{M}_\mathrm{A} = \left[\begin{array}{c|c} \mathsf{C}_5 & \mathsf{P} \\ \hline \mathsf{P}^\mathsf{T} & \mathsf{C}_5 \end{array}\right]$ and $\mathsf{M}_\mathrm{B} = \left[\begin{array}{c|c} \mathsf{C}_5 & 0 \\ \hline 0 & \mathsf{C}_5' \end{array}\right]$, for a certain permutation matrix P.

The two graphs have overlapping edges and different degrees. This is unwanted for our applications and may be

[5]Note that $\mathcal{E}$ and $\mathcal{Q}$ strictly speaking are allowed to be multisets as we allow parallel edges and multiple squares with the same boundary. The square complexes we construct here will only have squares of this type if there are parallel edges in the graphs used.

remedied, for example, in the following way. First, add self-loops to all vertices of the second graph to make their degrees equal. Then, take two copies of the resulting graph, and use the bipartite double cover of the Petersen graph (the Desargues graph [40]), as explained in Section III-C. If one in the end also wants both graphs to be bipartite on the same partition of vertices, one may take the bipartite double cover of both resulting graphs.

B. New Construction

1) General Case: Let $\mathscr{G}_\mathrm{A} = (\mathcal{V}, \mathcal{E}_\mathrm{A})$ and $\mathscr{G}_\mathrm{B} = (\mathcal{V}, \mathcal{E}_\mathrm{B})$ be (undirected) commuting Δ-regular graphs with no overlapping edges and a chosen partition $\mathcal{V} = \mathcal{V}_0 \sqcup \mathcal{V}_1$ for which both graphs are bipartite. We treat the graphs as digraphs with labelings $\eta_\mathrm{A} : \mathcal{E}_\mathrm{A}^{\mathrm{dir}} \to \mathcal{A}$ and $\eta_\mathrm{B} : \mathcal{E}_\mathrm{B}^{\mathrm{dir}} \to \mathcal{B}$, respectively. Furthermore, assume that if two vertices v, w are connected by an edge in $\mathscr{G}_\mathrm{A}$, then the sets of pairs of "inverses" for the two vertices are equal, meaning $\{(\eta_\mathrm{B}(\vec{e}), \eta_\mathrm{B}(\overleftarrow{e})) : e \in \mathcal{E}_\mathrm{B}(v)\} = \{(\eta_\mathrm{B}(\vec{e}), \eta_\mathrm{B}(\overleftarrow{e})) : e \in \mathcal{E}_\mathrm{B}(w)\}$, and vice versa when swapping the role of A and B. When this holds, we will say the graphs have locally invertible labels.

From the commuting graphs $\mathscr{G}_\mathrm{A}, \mathscr{G}_\mathrm{B}$, we may construct a square complex $\mathcal{X}$ with vertices $\mathcal{V}$, edges $\mathcal{E}_\mathrm{A} \cup \mathcal{E}_\mathrm{B}$, and for each $v \in \mathcal{V}_0$, $a \in \mathcal{A}$, and $b \in \mathcal{B}$, a square $(e_1, e_2, e_3, e_4) \in \mathcal{E}_\mathrm{A} \times \mathcal{E}_\mathrm{A} \times \mathcal{E}_\mathrm{B} \times \mathcal{E}_\mathrm{B}$ given by (1) below. We illustrate it by the square on the left when $t(\vec{e}_1) = (w, 1)$, $t(\vec{e}_3) = (w', 1)$, $s(\vec{e}_2) = (v', 0)$, $\eta_\mathrm{A}(\vec{e}_1) = a$, and $\eta_\mathrm{B}(\vec{e}_3) = b$.

$$\begin{array}{ccc} (w',1) & \xrightarrow[\overleftarrow{e}_2]{a} & (v',0) \\ {\scriptstyle b}\uparrow{\scriptstyle \vec{e}_3} & & {\scriptstyle b}\uparrow{\scriptstyle \overleftarrow{e}_4} \\ (v,0) & \xrightarrow[\vec{e}_1]{a} & (w,1) \end{array} \qquad \begin{cases} s(\vec{e}_1) = s(\vec{e}_3) = (v,0), \\ \eta_\mathrm{A}(\vec{e}_1) = \eta_\mathrm{A}(\overleftarrow{e}_2),\ s(\overleftarrow{e}_2) = t(\vec{e}_3), \\ \eta_\mathrm{B}(\vec{e}_3) = \eta_\mathrm{B}(\overleftarrow{e}_4),\ s(\overleftarrow{e}_4) = t(\vec{e}_1). \end{cases} \quad (1)$$

The squares (e_1, e_2, e_3, e_4) and (e_2, e_1, e_4, e_3) are identified. We denote the set of squares of $\mathcal{X}$ by $\mathcal{Q}$.

We define $\mathscr{G}_0^\square = (\mathcal{V}_0, \mathcal{E}_0^\mathcal{Q})$ as the Δ^2-regular graph with vertices $\mathcal{V}_0$ and an edge $(v, v') \in \mathcal{E}_0^\mathcal{Q}$ labeled by $(\eta_\mathrm{A}(\vec{e}_1), \eta_\mathrm{B}(\vec{e}_3)) = (a, b) \in \mathcal{A} \times \mathcal{B}$ in the local view of v and $(\eta_\mathrm{A}(\vec{e}_2), \eta_\mathrm{B}(\vec{e}_4))$ in the local view of v', for each square on the form (1). Similarly, we let $\mathscr{G}_1^\square = (\mathcal{V}_1, \mathcal{E}_1^\mathcal{Q})$ be the Δ^2-regular graph with vertices $\mathcal{V}_1$ and an edge (w, w') labeled $(\eta_\mathrm{A}(\overleftarrow{e}_1), \eta_\mathrm{B}(\overleftarrow{e}_4))$ in the local view of w and $(\eta_\mathrm{A}(\overleftarrow{e}_2), \eta_\mathrm{B}(\overleftarrow{e}_3))$ in the local view of w' for each square on the form (1).

Remark 3. *A bipartite graph $\mathscr{G} = (\mathcal{V}_0 \sqcup \mathcal{V}_1, \mathcal{E})$ gives rise to graphs $(\mathcal{V}_0, \mathcal{E}_0^2)$ and $(\mathcal{V}_1, \mathcal{E}_1^2)$, called the bipartite halves of $\mathscr{G}$, where we have an edge (v, v') in $\mathcal{E}_i^2$ for each (unordered) pair of edges $(v, w), (w, v')$ in $\mathscr{G}$ with $w \in \mathcal{V}_{i+1}$ (addition mod 2). The graphs $\mathscr{G}_0^\square$ and $\mathscr{G}_1^\square$ are the subgraphs of the two bipartite halves of $\mathscr{G}_\mathrm{A} \cup \mathscr{G}_\mathrm{B}$ where all edges come from pairs e_0, e_1 with $e_0 \in \mathscr{G}_\mathrm{A}, e_1 \in \mathscr{G}_\mathrm{B}$.*

Definition 10. *Given graphs as above and classical codes $\mathscr{C}_\mathrm{A}$, $\mathscr{C}_\mathrm{B}$ of length Δ, define $\mathscr{C}_0$ and $\mathscr{C}_1$ as the Tanner codes*

$$\mathscr{C}_0 = \mathrm{Tan}(\mathscr{G}_0^\square, (\mathscr{C}_\mathrm{A} \otimes \mathscr{C}_\mathrm{B})^\perp),\ \mathscr{C}_1 = \mathrm{Tan}(\mathscr{G}_1^\square, (\mathscr{C}_\mathrm{A}^\perp \otimes \mathscr{C}_\mathrm{B}^\perp)^\perp).$$

See Appendix B in the supplementary material for a concrete construction of parity-check matrices for the codes $\mathscr{C}_0$ and $\mathscr{C}_1$ from Definition 10.

Proposition 3 below is proved similarly to the corresponding statement in [9].

Proposition 3. *The codes $\mathscr{C}_0$ and $\mathscr{C}_1$ form a CSS code which is also a quantum LDPC code.*

Proof: Appendix A-B in the supplementary material. ∎

Remark 4. *Two Schreier graphs commute precisely when the group actions $\mathcal{G}_\mathrm{A} \times \mathcal{V} \to \mathcal{V}$ and $\mathcal{G}_\mathrm{B} \times \mathcal{V} \to \mathcal{V}$ defining them form a group action $\mathcal{G}_\mathrm{A} \times \mathcal{G}_\mathrm{B} \times \mathcal{V} \to \mathcal{V}$. Hence, providing a group action $\mathcal{G}_\mathrm{A} \times \mathcal{G}_\mathrm{B} \times \mathcal{V} \to \mathcal{V}$ and subsets $\mathcal{A} \subseteq \mathcal{G}_\mathrm{A}, \mathcal{B} \subseteq \mathcal{G}_\mathrm{B}$ is equivalent to providing commuting Schreier graphs* $\mathrm{Sch}(\mathcal{G}_\mathrm{A}, \mathcal{V}, \mathcal{A})$ *and* $\mathrm{Sch}(\mathcal{G}_\mathrm{B}, \mathcal{V}, \mathcal{B})$.

2) Symmetric Labeling Set: The construction used in Definition 10 can be somewhat simplified when the labeling sets are symmetric. In this case, the inverse of each label is well-defined. When the graphs involved are not already bipartite (with respect to the same partition of vertices), we can make them so by using the bipartite double cover of the graphs, simplifying it further. In this case, $\mathscr{G}_0^\square = \mathscr{G}_1^\square$.

C. Connection With Previous Constructions

To create commuting graphs $\mathscr{G}_\mathrm{A}, \mathscr{G}_\mathrm{B}$, one may start with a group $\mathcal{G}$ and two symmetric subsets $\mathcal{A}, \mathcal{B} \subseteq \mathcal{G}$. Then the Cayley graphs $\mathscr{G}_\mathrm{A} = \mathrm{Cay}_\mathrm{l}(\mathcal{G}, \mathcal{A})$ and $\mathscr{G}_\mathrm{B} = \mathrm{Cay}_\mathrm{r}(\mathcal{G}, \mathcal{B})$ will commute because group multiplication is associative. Our construction on the bipartite double covers of these graphs is equivalent to the approach used to create quantum Tanner codes so far [9].

Our assumption that the graphs $\mathscr{G}_\mathrm{A}, \mathscr{G}_\mathrm{B}$ have no overlapping edges plays the same role as the total no-conjugacy (TNC) condition for the quantum Tanner codes defined on groups, which states that $ag \neq gb$ for all $g \in \mathcal{G}, a \in \mathcal{A}, b \in \mathcal{B}$. It ensures that v and v' in (1) are different so that there are no self-loops in $\mathscr{G}_0^\square, \mathscr{G}_1^\square$. Many authors use "the quadripartite construction" to avoid dealing with the TNC condition.

In our setup, the quadripartite construction corresponds to the regular construction on two copies of one of the graphs and the bipartite double cover of the other. In other words, for graphs with adjacency matrices M_A and M_B, use the graphs with adjacency matrices

$$\left[\begin{array}{c|c} 0 & \mathsf{M}_\mathrm{A} \\ \hline \mathsf{M}_\mathrm{A} & 0 \end{array}\right] \quad \text{and} \quad \left[\begin{array}{c|c} \mathsf{M}_\mathrm{B} & 0 \\ \hline 0 & \mathsf{M}_\mathrm{B} \end{array}\right].$$

It can easily be seen that the two graphs still commute after this step when the obvious labeling is chosen. In the case of Cayley graphs, one may equivalently swap the group $\mathcal{G}$ for $\mathcal{G} \times \mathbb{F}_2$, and use $\mathcal{A}' = \{(a, 1) : a \in \mathcal{A}\}$ and $\mathcal{B}' = \{(b, 0) : b \in \mathcal{B}\}$. This means that using the quadripartite construction is quite restrictive when looking for concrete finite-length examples.

The following proposition should be clear when comparing our construction with the one from [9].

Proposition 4. *Let $\mathcal{G}$ be a group with generating symmetric subsets $\mathcal{A}$ and $\mathcal{B}$ of size Δ satisfying the TNC condition and not containing the neutral element, and let $\mathscr{C}_\mathrm{A}, \mathscr{C}_\mathrm{B}$ be codes of length Δ. Then, our construction applied to the bipartite double covers of the graphs* $\mathrm{Cay}_\mathrm{l}(\mathcal{G}, \mathcal{A}), \mathrm{Cay}_\mathrm{r}(\mathcal{G}, \mathcal{B})$ *and the*

codes $\mathscr{C}_\mathrm{A}, \mathscr{C}_\mathrm{B}$ gives the same CSS code as the construction from [9] applied to $\mathcal{G}, \mathcal{A}, \mathcal{B}, \mathscr{C}_\mathrm{A}, \mathscr{C}_\mathrm{B}$.

From Proposition 1, most regular graphs can be used to construct quantum Tanner codes. However, to have freedom when choosing the other graph, the automorphism group of the graph should be large. Moving away from Cayley graphs means getting a smaller automorphism group, see Section IV.

D. Equivalent Characterizations

It is natural to ask when a square complex can give CSS codes the way left-right Cayley complexes and our square complexes described in Section III-B do, namely, by changing which diagonal of the squares that determines their endpoints when viewed as edges. Since we are placing constraints on the edges according to tensor products of codes of length Δ, we restrict ourselves to square complexes where each vertex has face degree $|\mathcal{A}| \times |\mathcal{B}| = \Delta^2$. We now turn to prove that these are precisely the square complexes that can be made from two commuting graphs (see Corollary 1). Along the way, we present another view of quantum Tanner codes (Lemma 3), and show how our construction fits in (Theorem 1).

In Lemma 3, we consider Δ^2-regular graphs. The local views are taken to be labeled by $\mathcal{A} \times \mathcal{B}$ for sets $\mathcal{A}, \mathcal{B}$ of size Δ so that the local view $\mathcal{E}(v)$ of a vertex v can be viewed as a matrix $\mathsf{E}(v)$ of size $\Delta \times \Delta$, where its entry $\mathsf{E}(v)_{a,b} = e \in \mathcal{E}$ when e is labeled (a, b) in $\mathcal{E}(v)$. Thus, the Tanner codes and the rows and columns of local views are well-defined.

Lemma 3. *Let $\mathscr{G}_0 = (\mathcal{V}_0, \mathcal{E}_0)$ and $\mathscr{G}_1 = (\mathcal{V}_1, \mathcal{E}_1)$ be Δ^2-regular graphs with local views labeled by $\mathcal{A} \times \mathcal{B}$ for sets $\mathcal{A}, \mathcal{B}$ of size Δ such that $|\mathcal{V}_0| = |\mathcal{V}_1|$, and let $\psi : \mathcal{E}_0 \to \mathcal{E}_1$ be the bijection given by the order on the edges. Then, (i) and (ii) are equivalent.*

- *(i) The Tanner codes $\mathscr{C}_0 = \mathrm{Tan}(\mathscr{G}_0, (\mathscr{C}_\mathrm{A} \otimes \mathscr{C}_\mathrm{B})^\perp)$ and $\mathscr{C}_1 = \mathrm{Tan}(\mathscr{G}_1, (\mathscr{C}_\mathrm{A}^\perp \otimes \mathscr{C}_\mathrm{B}^\perp)^\perp)$ form a CSS code for all classical codes $\mathscr{C}_\mathrm{A}, \mathscr{C}_\mathrm{B}$ of length Δ.*
- *(ii) For any vertices $v \in \mathcal{V}_0, w \in \mathcal{V}_1$, either $\mathcal{U} \triangleq \psi(\mathcal{E}_0(v)) \cap \mathcal{E}_1(w) = \emptyset$, or $\mathcal{U}$ forms one or more rows or columns in the local views matrix $\mathsf{E}_1(w)$, such that each row (column) is mapped by ψ^{-1} to a row (column) in $\mathsf{E}_0(v)$.*

We find it reasonable to call any codes $\mathscr{C}_0, \mathscr{C}_1$ constructed as in (i) *general quantum Tanner codes*, so these codes fit in the red region of Fig. 1. Note that Δ^m-regular graphs with m local codes $\mathscr{C}_{\mathrm{A}_1}, \ldots, \mathscr{C}_{\mathrm{A}_m}$ also are of interest and could share this name. However, we restrict ourselves to the case $m = 2$.

Proof: Without loss of generality, let $\mathcal{A} = \{a_1, \ldots, a_\Delta\}$ and $\mathcal{B} = \{b_1, \ldots, b_\Delta\}$. Next, let v, w be vertices such that $\psi(\mathcal{E}_0(v)) \cap \mathcal{E}_1(w) = \mathcal{U} \neq \emptyset$. Recall that $\mathscr{C}_0^\perp$ is the span of all $(\mathscr{C}_\mathrm{A} \otimes \mathscr{C}_\mathrm{B})$-generators for $\mathscr{C}_0$, while $\mathscr{C}_1$ is the space orthogonal to the $(\mathscr{C}_\mathrm{A}^\perp \otimes \mathscr{C}_\mathrm{B}^\perp)$-generators for $\mathscr{C}_1$. Since (i) holds, i.e., $\mathscr{C}_0^\perp \subseteq \mathscr{C}_1$, this tells us that the $(\mathscr{C}_\mathrm{A} \otimes \mathscr{C}_\mathrm{B})$-generators for $\mathscr{C}_0$ are orthogonal to the $(\mathscr{C}_\mathrm{A}^\perp \otimes \mathscr{C}_\mathrm{B}^\perp)$-generators for $\mathscr{C}_1$, meaning a codeword of $(\mathscr{C}_\mathrm{A} \otimes \mathscr{C}_\mathrm{B})$ restricted to $\psi^{-1}(\mathcal{U}) \subseteq \mathcal{E}_0(v)$ must be orthogonal to a codeword of $(\mathscr{C}_\mathrm{A}^\perp \otimes \mathscr{C}_\mathrm{B}^\perp)$ restricted to $\mathcal{U}$ regardless of $\mathscr{C}_\mathrm{A}$ and $\mathscr{C}_\mathrm{B}$. With our choice of local codes, this implies that $\mathcal{U}$ is labeled by a set of the form $\{(a_i, b_j) : i \in [\Delta], j \in \mathcal{J}\}$ (or $\{(a_i, b_j) : i \in \mathcal{I}, j \in [\Delta]\}$) in $\mathcal{E}_1(w)$, for some $\mathcal{J}$ (or $\mathcal{I}$) $\subseteq [\Delta]$, and $\psi^{-1}(\mathcal{U})$ is labeled by $\{(a_i, b_{j'}) : i \in [\Delta], j' \in \mathcal{J}'\}$ (or $\{(a_{i'}, b_j) : i' \in \mathcal{I}', j \in [\Delta]\}$) in $\mathcal{E}_0(v)$, for some $\mathcal{J}'$ (or $\mathcal{I}'$) $\subseteq [\Delta]$ of the same size as $\mathcal{J}$ (or $\mathcal{I}$). In the first case, the edges must "line up" so that the edge labeled $(a_i, b_{j'})$ in $\psi^{-1}(\mathcal{U})$ is mapped to the edge labeled (a_i, b_j) in $\mathcal{E}_1(w)$ by ψ (mapping columns). In the other case ψ must map the edge labeled $(a_{i'}, b_j)$ to the edge labeled (a_i, b_j) (mapping rows).

To prove that (ii) implies (i) we proceed as follows. Let $\boldsymbol{v}$ be a $(\mathscr{C}_\mathrm{A} \otimes \mathscr{C}_\mathrm{B})$-generator for $\mathscr{C}_0$, and let $\boldsymbol{w}$ be a $(\mathscr{C}_\mathrm{A}^\perp \otimes \mathscr{C}_\mathrm{B}^\perp)$-generator for $\mathscr{C}_1$, supported at $\mathcal{E}_0(v)$ and $\mathcal{E}_1(w)$, respectively. We want to show that $\boldsymbol{v}$ and $\boldsymbol{w}$ are orthogonal to each other so that $\mathscr{C}_0$ and $\mathscr{C}_1$ form a CSS code. Suppose, without loss of generality, that $\mathcal{U}$ is labeled by $\{(a_i, b_j) : i \in \mathcal{I}, j \in [\Delta]\}$ in $\mathcal{E}_1(w)$, for some $\mathcal{I} \subseteq [\Delta]$, and $\psi^{-1}(\mathcal{U})$ is labeled by $\{(a_{i'}, b_j) : i' \in \mathcal{I}', j \in [\Delta]\}$ in $\mathcal{E}_0(v)$, for some $\mathcal{I}' \subseteq [\Delta]$ of the same size as $\mathcal{I}$, mapped by ψ as above. The generator $\boldsymbol{v}$ is now a codeword of $\mathscr{C}_\mathrm{B}$ on the set of edges labeled by $\{(a_{i'}, b_j) : j \in [\Delta]\}$ in $\mathcal{E}_0(v)$ for each $i' \in \mathcal{I}'$, while $\boldsymbol{w}$ is a codeword of $\mathscr{C}_\mathrm{B}^\perp$ on the image of each of these sets of edges by ψ, and it follows that $\boldsymbol{v}$ and $\boldsymbol{w}$ are orthogonal. ∎

Theorem 1 gives a condition that restricts the codes constructed in Lemma 3 from the red region of Fig. 1 to the green region.

Theorem 1. *Let $\mathscr{G}_0$, $\mathscr{G}_1$, and ψ be as in Lemma 3. Then, (i) and (ii) of Lemma 3 are equivalent to (iii) below if and only if the following holds for each edge e in $\mathscr{G}_0$. For each label e and $\psi(e)$ have in common, the labels of e share one index in the labeling set $\Delta \times \Delta$.*

- *(iii) There exist commuting $\mathscr{G}_\mathrm{A} = (\mathcal{V}, \mathcal{E}_\mathrm{A})$, $\mathscr{G}_\mathrm{B} = (\mathcal{V}, \mathcal{E}_\mathrm{B})$ for $\mathcal{V} \triangleq \mathcal{V}_0 \sqcup \mathcal{V}_1$ such that $\mathscr{G}_i^\square$ constructed from $\mathscr{G}_\mathrm{A}, \mathscr{G}_\mathrm{B}$ as in Section III-B, equals $\mathscr{G}_i$ for $i = 0, 1$.*

We refer to the condition on ψ mentioned in Theorem 1 as *the swapping condition*, where the name comes from Lemma 4 below. We need this lemma and one more (Lemma 5) to prove Theorem 1, so we state them before turning to the proof of the theorem.

Lemma 4. *Let $\mathscr{G}_0$, $\mathscr{G}_1$, and ψ as in Lemma 3 satisfying the swapping condition be given. Then, an edge in $\mathscr{G}_0$ corresponding to (a, b) and (a', b') in its local views must be mapped by ψ to an edge corresponding to (a, b') and (a', b) in its local views.*

Proof: Condition (ii) of Lemma 3 implies that a, b, a', b' all need to be possible to fix individually, so the only other option is ψ fixing the labels, in which case the swapping condition of Theorem 1 tells us that $a' = a$ and $b' = b$. ∎

Lemma 5. *Let $\mathscr{G}_0$, $\mathscr{G}_1$, and ψ as in Lemma 3 satisfying the swapping condition be given, and let $(v, v') \in \mathcal{E}_0$ be an edge labeled (a, b) in $\mathcal{E}_0(v)$ and (a', b') in $\mathcal{E}_0(v')$. The edges in the local view of v with a as the first entry of their label will then have a' as the first entry of the label in their other local view. Similarly, the edges of $\mathcal{E}_0(v)$ having b as the second entry of their label will have b' as the second entry of their label in their other local view.*

Proof: The image of a set of edges $\{e_i\}$ forming a row in $\mathsf{E}_0(v)$ has to form a row (in the same order as before) in some local view after being mapped by ψ. For $\{\psi(e_i)\}$ to form a row in this way, the second entry of their label must be the same as it is in $\mathsf{E}_0(v)$, and the first entry of the label must be common for all the edges. By the swapping condition, this entry is precisely the first entry of the labels of the edges in $\{e_i\}$ in their other local view (i.e., not the local view of v, but of their other endpoint). ∎

Proof of Theorem 1: We have already shown that (iii) implies (i) in Proposition 3, and (i) and (ii) are equivalent by Lemma 3. Theorem 1 says that (ii) implies (iii) precisely when the swapping condition is satisfied. As a diagram, what we want to show is that the gray implication arrow below holds precisely when the swapping condition is satisfied.

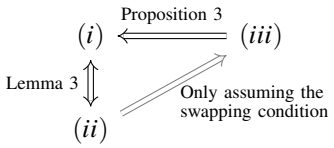

We will first show the only-if part of the theorem by showing that all ψ coming from our construction will satisfy the swapping condition. Then, we show the if-part of the theorem by constructing $\mathscr{G}_\mathrm{A}$ and $\mathscr{G}_\mathrm{B}$ as in (iii) assuming the swapping condition. Lemmas 4 and 5 will be used to show that the construction is well-defined.

We now prove the only-if part of the theorem by showing that the swapping condition will be satisfied whenever (iii) is satisfied by the following argument. An edge in $\mathscr{G}_0^\square$ coming from the square

$$\begin{array}{ccc} (w',1) & \xrightarrow{e_2} & (v',0) \\ {\scriptstyle e_3}\big| & & \big|{\scriptstyle e_4} \\ (v,0) & \xrightarrow{e_1} & (w,1) \end{array}$$

corresponds to the edge in $\mathscr{G}_1^\square$ coming from the same square. Recall that we for a bipartite graph with vertices $\mathcal{V}_0 \sqcup \mathcal{V}_1$ let $\eta(\vec{e})$ denote the label of e in the local view of its endpoint with second index 0. In $\mathscr{G}_0^\square$ it has the labels $(\eta(\vec{e}_1),\eta(\vec{e}_3))$ and $(\eta(\vec{e}_2),\eta(\vec{e}_4))$, and in $\mathscr{G}_1^\square$ it has the labels $(\eta(\vec{e}_2),\eta(\vec{e}_3))$ and $(\eta(\vec{e}_1),\eta(\vec{e}_4))$. So if one of the two labels the edge has in $\mathscr{G}_0^\square$ is equal to a label of the edge in $\mathscr{G}_1^\square$, this implies that either $\eta(\vec{e}_1)=\eta(\vec{e}_2)$ or $\eta(\vec{e}_3)=\eta(\vec{e}_4)$, and if both labels are equal we have both $\eta(\vec{e}_1)=\eta(\vec{e}_2)$ and $\eta(\vec{e}_3)=\eta(\vec{e}_4)$. This means that the ψ we get from our construction in Section III satisfies the swapping condition, proving the only-if part of Theorem 1.

Next, we prove the if-part of the theorem. In particular, we show that (ii) implies (iii) given the swapping condition, i.e., that the swapping condition is not only necessary to satisfy (iii), but also sufficient.

We do this by constructing a square complex in the following way. Given an edge (v,v') labeled (a,b) in $\mathcal{E}_0(v)$ and (a',b') in $\mathcal{E}_0(v')$ mapped by ψ to an edge (w,w'), Lemma 4 tells us that we may assume the edges are labeled (a',b) in $\mathcal{E}_1(w)$ and (a,b') in $\mathcal{E}_1(w')$. For each such edge, we make the square

$$\begin{array}{ccc} (w',1) & \underset{a'}{\overset{a}{\rightleftarrows}} & (v',0) \\ {\scriptstyle b}\uparrow\downarrow{\scriptstyle b'} & q & {\scriptstyle b}\uparrow\downarrow{\scriptstyle b'} \\ (v,0) & \underset{a'}{\overset{a}{\rightleftarrows}} & (w,1), \end{array}$$

meaning four vertices, four edges labeled in each direction as indicated, and one square glued onto them.

Below is an example picture, where the fat blue edge (v_1,v_4) is mapped to the fat red edge (w_3,w_4), giving rise to the gray square $(((v_1,0),(w_3,1)),((v_4,0),(w_4,1)),((v_1,0),(w_4,1)),((v_4,0),(w_3,1)))$.

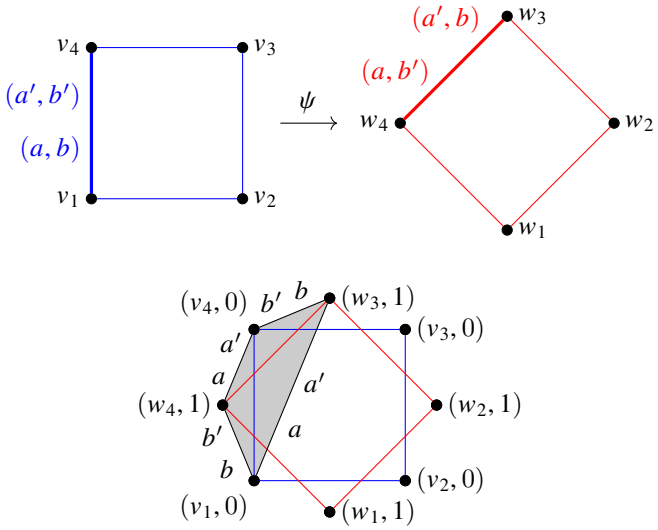

Next, equal vertices are identified, and so are edges with equal labels between equal vertices. From Lemma 5, it follows that given a vertex v and an element $x \in \mathcal{A}\cup\mathcal{B}$, we will have exactly one edge in the local view of v labeled x after this identification. We obtain a square complex $\mathcal{X}$ with vertices $\mathcal{V}_0 \sqcup \mathcal{V}_1$, where the underlying graph is bipartite with local views labeled by $\mathcal{A}\cup\mathcal{B}$, and squares on the above form. This underlying graph may be split into two graphs with labeling set $\mathcal{A}$ and $\mathcal{B}$, respectively. It is clear that we get back the same square complex $\mathcal{X}$ when doing the construction described in Section III-B on these two graphs, and that the diagonals of the squares in this square complex are precisely the edges of $\mathscr{G}_0$ and $\mathscr{G}_1$ that correspond to each other. Hence, (iii) holds. ∎

Corollary 1. *Let graphs $\mathscr{G}_0^\square,\mathscr{G}_1^\square$ satisfying (i) of Lemma 3 be given. If the edges of $\mathscr{G}_0^\square$ are (some) diagonals of squares in a square complex and $\mathscr{G}_1^\square$ is the graph of opposite diagonals, then the graphs $\mathscr{G}_0^\square,\mathscr{G}_1^\square$ can be constructed from a pair of commuting graphs as in Section III-B.*

Proof: Since ψ is constructed by changing the diagonal of a square complex, the swapping condition is satisfied by the proof of the only-if part of Theorem 1. Therefore, the result follows from Theorem 1. ∎

We give an easy example showing the existence of cases where condition (i) of Lemma 3 holds but the swapping condition of Theorem 1 does not. This indicates that the red

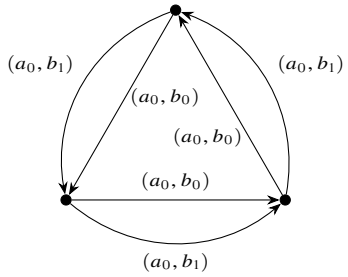

Fig. 3. The depicted graph is considered in Example 2, drawn according to the convention from Example 1. It is 4-regular with edges depicted as arrows. An edge has the indicated label in the local view of the source of the arrow depicting it. An edge labeled (a_0, b_0) in one of its local views is labeled (a_1, b_0) in the other, and similarly the "inverse" of (a_0, b_1) is (a_1, b_1).

region of Fig. 1 is strictly larger than the green one, even when restricting ourselves to the local codes we use here.

Example 2. *Fig. 3 shows a 4-regular graph $\mathscr{G}$ with local views labeled by $\{a_0, a_1\} \times \{b_0, b_1\}$ such that an edge labeled (a_0, b_i) in one local view is labeled (a_1, b_i) in the other, for $i \in \{0, 1\}$. Using $\mathscr{G}_0 = \mathscr{G}_1 = \mathscr{G}$ as the depicted graph and $\psi = \mathrm{id}$, where* id *denotes the identity mapping, (ii) is satisfied by the following observation. Two overlapping local views can either be local views of the same vertex or of neighboring vertices. In the first case, it can be viewed as either two columns or two rows, and in the second, it is the first row of one of the local views and the second row of the other. However, ψ fixes both labels of each edge, and only the second index is shared in the two labels of each edge, meaning that the swapping condition of Theorem 1 is not satisfied.*

Remark 5. *Example 2 can be viewed as an example of a construction where each edge in a Δ-regular graph $\mathscr{G}$ is swapped for Δ parallel edges given a labeling such that $\psi = \mathrm{id}$ satisfies condition (ii) of Lemma 3. Hence, these Δ^2-regular graphs can be used to make general quantum Tanner codes. The graph may also be constructed as $\mathscr{G}_0^{\square} = \mathscr{G}_1^{\square}$ using $\mathscr{G}_\mathrm{A} = \mathscr{G}$ and a graph of only (self-inverse) self-loops as $\mathscr{G}_\mathrm{B}$. However, not every labeling of the graph that would satisfy (ii) may be constructed using the construction from Section III-B, as Example 2 shows.*

IV. Asymptotically Good Quantum Codes

In this section, we construct an asymptotically good family of quantum LDPC codes using our proposed construction. We use non-Cayley graphs, placing us in the blue region of Fig. 1. This is summed up in the following theorem.

Theorem 2. *Let $\Delta = 2q+2$ for a prime q be given. There exists an infinite family of pairs of commuting Δ-regular Schreier graphs $\mathscr{G}_\mathrm{A}$, $\mathscr{G}_\mathrm{B}$ where $\mathscr{G}_\mathrm{A}$ is non-Cayley and the following holds. If Δ is large enough, then, for any $\rho \in (0, 1/2)$ and $\delta > 0$ satisfying $-\delta \log_2 \delta - (1-\delta)\log_2(1-\delta) < \rho$, there exists a $\kappa > 0$ such that, with nonzero probability, randomly choosing local codes $\mathscr{C}_\mathrm{A}, \mathscr{C}_\mathrm{B}$ of length Δ and rates ρ and $1-\rho$, respectively, gives, for any pair $\mathscr{G}_\mathrm{A}, \mathscr{G}_\mathrm{B}$ in the family, a quantum LDPC code of length $n = |\mathcal{V}|\Delta^2$ (where $\mathcal{V}$ is the vertex set of $\mathscr{G}_\mathrm{A}$ and $\mathscr{G}_\mathrm{B}$), rate $k/n \geq (2\rho-1)^2$, and minimum distance $d \geq \frac{\delta^2\kappa^2 n}{2 \cdot 1024 \Delta}$.*

The graphs are not already bipartite, and will be made so by taking their bipartite double cover. Since $\mathscr{G}_0^{\square}$ and $\mathscr{G}_1^{\square}$ then are isomorphic, we will write $\mathscr{G}^{\square}$ for both to lighten notation. We start by stating Proposition 5 below, which gives an obstruction for when a pair of commuting graphs can be non-Cayley.

Note that Proposition 5 considers Cayley graphs that allow for multiplicities in the set $\mathcal{A}$ of Definition 2, where Cayley graphs are defined. Also, recall that we do not demand $\mathcal{A}$ to be generating the group, so we allow Cayley graphs to have more than one connected component.

Proposition 5. *If $\mathscr{G}_\mathrm{A}$ and $\mathscr{G}_\mathrm{B}$ commute and have locally invertible labels, then they are either both Cayley graphs or one of them has more than one component.*

Proof: Let $\mathscr{G}_\mathrm{A}$ and $\mathscr{G}_\mathrm{B}$ be connected commuting graphs. Since they are connected, they have invertible labels, and therefore each label defines a permutation on the vertices. According to Lemma 1, when a permutation π_b commutes with a set of permutations $\{\pi_a : a \in \mathcal{A}\}$, this is equivalent to the permutation being a graph homomorphism of the graph $\mathscr{G}_\mathrm{A} = \mathrm{Sch}(\mathcal{G}(\mathcal{A}), \mathcal{V}, \mathcal{A})$, where $\mathcal{G}(\mathcal{A})$ is the group generated by $\mathcal{A}$. The graph $\mathscr{G}_\mathrm{A}$ is connected, so the action of $\mathcal{G}(\mathcal{A})$ on $\mathcal{V}$ is transitive. Moreover, since the graphs commute, all π_b must be elements of $\mathrm{Aut}_{\mathcal{G}(\mathcal{A})}(\mathcal{V})$, and because the graph $\mathscr{G}_\mathrm{B}$ is connected, $\mathrm{Aut}_{\mathcal{G}(\mathcal{A})}(\mathcal{V})$ therefore acts transitively. Assuming the action of $\mathcal{G}(\mathcal{A})$ on $\mathcal{V}$ is also faithful, Proposition 2 now tells us that $\mathcal{G}(\mathcal{A})$ must act regularly on $\mathcal{V}$.

If the group action of $\mathcal{G}(\mathcal{A})$ on $\mathcal{V}$ is not faithful, then, because the labeling set for graphs with locally invertible labels will be symmetric if the graphs are connected, the group elements that act the same way on $\mathcal{V}$ can be viewed as several copies of the same group element, making the group action faithful.

A Schreier graph $\mathrm{Sch}(\mathcal{G}, \mathcal{V}, \mathcal{A})$ defined by a regular group action $\mathcal{G} \times \mathcal{V} \to \mathcal{V}$ must be a Cayley graph in the sense of Remark 1 by the following argument. Fix a vertex $v_0 \in \mathcal{V}$, and let $g_v \in \mathcal{G}$ for $v \in \mathcal{V}$ be the unique group element such that $g_v v_0 = v$. Now, give the set $\mathcal{V}$ a group structure by letting $v \cdot w = g_v g_w$. The group $(\mathcal{V}, \cdot)$ is now isomorphic to $\mathcal{G}$, and this isomorphism takes the group action to group multiplication. ∎

At first glance, it might seem like Proposition 5 tells us there is no hope of finding asymptotically good quantum codes using the methods from [9] or [28]. After all, the spectral expansion of the graphs involved is a very important tool in both of these papers (as well as for other constructions of good quantum LDPC codes). If a Δ-regular digraph $\mathscr{G}$ has more than one component, its spectral expansion becomes $\lambda(\mathscr{G}) = \Delta$, which is as large as it can get. In [9] and [28] all graphs are therefore connected. However, we saw in Section III-C that the quadripartite construction is equivalent to the regular one, where one graph is replaced by its bipartite double cover and the other one by two copies of itself. Recalling that [28] uses the quadripartite construction, one can clearly get good codes even when $\mathscr{G}_\mathrm{A}$ or $\mathscr{G}_\mathrm{B}$ is disconnenced. This stems from the fact that $\mathscr{G}^{\square}$ and the components of $\mathscr{G}_\mathrm{A}$ and $\mathscr{G}_\mathrm{B}$ may have a small λ.

Since the adjacency matrices M_A and M_B are symmetric and

commute, they are simultaneously diagonalizable. Therefore, $\mathsf{M}_\mathrm{A} + \mathsf{M}_\mathrm{B}$ and $\mathsf{M}_\mathrm{A}\mathsf{M}_\mathrm{B}$, which are the adjacency matrices of, respectively, $(\mathcal{V}, \mathcal{E}_\mathrm{A} \cup \mathcal{E}_\mathrm{B})$ and $\mathscr{G}^{\square}$, have eigenvalues the sums and products, respectively, of the eigenvalues of M_A and M_B. To get a bound on $\lambda(\mathscr{G}^{\square})$ when $\mathscr{G}_\mathrm{A}$ and/or $\mathscr{G}_\mathrm{B}$ has several components, we need to say something about which eigenvalues from the two graphs will be multiplied together to make an eigenvalue of $\mathscr{G}^{\square}$. Proposition 6 gives a situation where we can do this, and generalizes the case from [1], where $\mathscr{G}_\mathrm{A}$ and $\mathscr{G}_\mathrm{B}$ with respectively one and two components were considered.

We will need the following observation and put it as a lemma for future reference. Here, for a graph $\mathscr{G}$ with local views labeled by $\mathcal{A}$, we say $a \in \mathcal{A}$ maps v to w if an edge (v, w) of $\mathscr{G}$ is labeled a in the local view of v.

Lemma 6. *If $\mathscr{G}_\mathrm{A}$ and $\mathscr{G}_\mathrm{B}$ commute and $a \in \mathcal{A}$ maps the vertex v to w in $\mathscr{G}_\mathrm{A}$, then all vertices in the component of $\mathscr{G}_\mathrm{B}$ containing v are mapped by a to vertices in the same component of $\mathscr{G}_\mathrm{B}$ as w.*

Proof: Given a vertex v' in $\mathscr{G}_\mathrm{B}$, it is in the same component as v if and only if there is a path of edges $(v, v_1), \ldots, (v_{m-1}, v')$ between $v_0 = v$ and $v_m = v'$. If the edge (v_i, v_{i+1}) is labeled b in the local view of v_i, then the commuting square starting in v_i given by a and b contains an edge of $\mathscr{G}_\mathrm{B}$ connecting the vertices that v_i and v_{i+1} are mapped to by a. ∎

Lemma 7. *Let $\mathscr{G}_\mathrm{A}$ and $\mathscr{G}_\mathrm{B}$ be commuting graphs. If two components of $\mathscr{G}_\mathrm{B}$ are connected by edges of $\mathscr{G}_\mathrm{A}$, then the two components are isomorphic.*

Proof: Let the i-th and j-th components of $\mathscr{G}_\mathrm{B}$ be connected by edges in $\mathscr{G}_\mathrm{A}$. Then there is some $a \in \mathcal{A}$ that sends a vertex in the j-th component to the i-th component, and a will have a local inverse $a' \in \mathcal{A}$. Therefore, Lemma 6 gives that the number of vertices in the two components are the same.

This means that the ij-th block A_{ij} of the adjacency matrix of $\mathscr{G}_\mathrm{A}$ is a square matrix. It is a sum of permutation matrices, one for each a that maps vertices in the j-th component of $\mathscr{G}_\mathrm{B}$ to the i-th component. Because $\mathscr{G}_\mathrm{A}$ commutes with $\mathscr{G}_\mathrm{B}$, each of these permutations must be a graph isomorphism between the components it connects. ∎

Proposition 6. *Let $\mathscr{G}_\mathrm{A}$ and $\mathscr{G}_\mathrm{B}$ be commuting graphs with underlying $m\Delta$-regular digraphs and adjacency matrices M_A and M_B, respectively, and suppose $\mathscr{G}_\mathrm{B}$ has m components. If the quotient graph of $\mathscr{G}_\mathrm{A}$, where vertices in the same component of $\mathscr{G}_\mathrm{B}$ are identified, is the graph where each pair of (not necessarily different) vertices has Δ parallel edges between them, then, among eigenvectors that simultaneously diagonalize the two adjacency matrices, all but one of the eigenvectors of M_B corresponding to $m\Delta$ will be eigenvectors corresponding to 0 for M_A.*

Proof: Let $\boldsymbol{u}$ be the all-ones vector (of suitable length). The $m\Delta$ eigenvalues of M_B will come from vectors of the form $\boldsymbol{v} = (\boldsymbol{v}_1, \ldots, \boldsymbol{v}_m)$ where $\boldsymbol{v}_i \in \{\boldsymbol{u}, -\boldsymbol{u}, \boldsymbol{0}\}$ for all $i \in [m]$. Let A_{ij} be the block of M_A that describes the edges of $\mathscr{G}_\mathrm{A}$ going from the j-th component of $\mathscr{G}_\mathrm{B}$ to the i-th component of $\mathscr{G}_\mathrm{B}$. Lemma 6 gives us that $\boldsymbol{u}$ is an eigenvector for each such block. The corresponding eigenvalue is precisely the number of $a \in \mathcal{A}$ taking vertices in the j-th component to the i-th component, or equivalently the number of parallel edges from the j-th vertex to the i-th vertex in the quotient graph of $\mathscr{G}_\mathrm{A}$ where vertices in the same component of $\mathscr{G}_\mathrm{B}$ are identified.

This means that all vectors $\boldsymbol{v}$ on the above form with an equal amount of $\boldsymbol{u}$ and $-\boldsymbol{u}$ present will correspond to the eigenvalue 0 in $\mathscr{G}_\mathrm{A}$.

The all-ones vector will correspond to $m\Delta$ for both graphs, and the multiplicity of $(m\Delta)^2$ must be 1 for the product $\mathsf{M}_\mathrm{A}\mathsf{M}_\mathrm{B}$ since $\mathscr{G}_\mathrm{A}$ connects all components of $\mathscr{G}_\mathrm{B}$ with each other. Therefore, the all-ones vector must be part of the basis of eigenvectors that simultaneously diagonalize the two adjacency matrices. The rest of the vectors in this basis will then be orthogonal to this vector. Because the components of $\mathscr{G}_\mathrm{B}$ by Lemma 7 have the same size, the eigenvectors $\boldsymbol{v}$ of M_B corresponding to $m\Delta$ are orthogonal to the all-ones vector precisely when the number of $\boldsymbol{u}$ and $-\boldsymbol{u}$ that appear in $\boldsymbol{v}$ are equal, and therefore correspond to the eigenvalue 0 for M_A. ∎

In the rest of this paper, we will only look at the case $m = 2$. Then we have two options, either $\mathscr{G}_\mathrm{A}$ is connected and $\mathscr{G}_\mathrm{B}$ is two isomorphic copies of a Cayley graph, or $\mathscr{G}_\mathrm{A}$ and $\mathscr{G}_\mathrm{B}$ both have two components. Either way, if $\mathscr{G}_\mathrm{B}$ has two components, then (each component of) $\mathscr{G}_\mathrm{A}$ can be viewed as the disjoint union of two Cayley graphs, connected by a bipartite Cayley graph. (The components of) $\mathscr{G}_\mathrm{A}$ will then have an adjacency matrix $\left[\begin{array}{c|c} \mathsf{A}_1 & \mathsf{A}_2 \\ \hline \mathsf{A}_2^\intercal & \mathsf{A}_3 \end{array}\right]$ where A_1 and A_3 are adjacency matrices for the first two Cayley graphs, while $\left[\begin{array}{c|c} 0 & \mathsf{A}_2 \\ \hline \mathsf{A}_2^\intercal & 0 \end{array}\right]$ is the adjacency matrix of the bipartite one. For now, we will consider the case where the bipartite graph is the bipartite double cover of a Cayley graph, so A_2 will be symmetric.

Remark 6. *If $\mathscr{G}_\mathrm{A}$ and $\mathscr{G}_\mathrm{B}$ are commuting (possibly not connected) left Cayley graphs, it is not necessarily true that one can be viewed as a right Cayley graph. Take, for example, $\mathcal{G} = \mathcal{G}_\mathrm{A} \times \mathcal{G}_\mathrm{B}$ to be the product of two non-abelian groups with generating sets $\mathcal{A}$ and $\mathcal{B}$, respectively. Then $\mathrm{Cay}_\mathrm{l}(\mathcal{G}, \mathcal{A} \times 1)$ and $\mathrm{Cay}_\mathrm{l}(\mathcal{G}, 1 \times \mathcal{B})$ will commute, but none of these graphs can be viewed as right Cayley graphs of $\mathcal{G}$. However, if one of the Cayley graphs is connected, then the labeling set of the other will only contain elements from the center of the group, and there will be no difference between the left and right multiplication of these elements.*

For our purposes, it will be sufficient to consider commuting Cayley graphs in the form of right Cayley graphs and left Cayley graphs, both in the rest of this section and in Section V. One should note that there possibly are applications where this is not desirable, for example, when constructing quantum locally testable codes using four commuting graphs [32]. However, when the graphs are connected, Proposition 5 and Remark 6 tell us that a commuting pair of connected graphs can always be viewed as one left and one right Cayley graph.

Proposition 7. *Let $\mathscr{G}_{\mathsf{A}_1}, \mathscr{G}_{\mathsf{A}_2}, \mathscr{G}_{\mathsf{A}_3}$ be connected graphs with Δ-regular underlying digraphs and adjacency matrices $\mathsf{A}_1, \mathsf{A}_2, \mathsf{A}_3$, respectively, and assume that $\mathscr{G}_{\mathsf{A}_2}$ is not bipartite so that its bipartite double cover will be connected. Then, the*

graph $\mathscr{G}$ with adjacency matrix $\left[\begin{array}{c|c} \mathsf{A}_1 & \mathsf{A}_2 \\ \hline \mathsf{A}_2 & \mathsf{A}_3 \end{array}\right]$ *will have* $\lambda(\mathscr{G}) \leq \lambda(\mathscr{G}_{\mathrm{A}_2}) + \max(\lambda(\mathscr{G}_{\mathrm{A}_1}), \lambda(\mathscr{G}_{\mathrm{A}_3}))$.

Proof: Appendix A-C in the supplementary material. ∎

For any left Cayley graph expander $\mathrm{Cay}_{\mathrm{l}}(\mathcal{G}, \mathcal{A})$ of a group $\mathcal{G}$ with a subgroup $\mathcal{H}$, the graph $\mathrm{Sch}(\mathcal{G}, \mathcal{G}/\mathcal{H}, \mathcal{A})$ will also be an expander. It is Cayley precisely when $\mathcal{H}$ is normal. The problem in our setting is that right multiplication respects the cosets if and only if $\mathcal{H} \subseteq \mathcal{G}$ is normal, so $\mathcal{B}$ cannot generate the whole group $\mathcal{G}$ if $\mathcal{H}$ is not normal and $\mathrm{Sch}(\mathcal{G}, \mathcal{G}/\mathcal{H}, \mathcal{B})$ is to be well-defined. The graph is well-defined precisely when the subgroup $\mathcal{G}_{\mathrm{B}} \subseteq \mathcal{G}$ generated by $\mathcal{B}$ satisfies that $\mathcal{H}$ is normal in $\mathcal{G}_{\mathrm{B}}$. This reflects Proposition 5, and the number of components in the second graph will be $|\mathcal{G}|/|\mathcal{G}_{\mathrm{B}}|$.

Proposition 7 lets us use a different approach, where we swap out a good expander $\mathscr{G}_{\mathrm{A}} = \mathrm{Cay}_{\mathrm{l}}(\mathcal{G}, \mathcal{A})$ with adjacency matrix A for the graph $\mathscr{G}$ with adjacency matrix $\mathsf{M}_{\mathrm{A}} = \left[\begin{array}{c|c} \mathsf{A} & \mathsf{A} \\ \hline \mathsf{A} & \mathsf{PAP}^{\mathsf{T}} \end{array}\right]$, where P is some permutation matrix given by multiplication by a group element $h \in \mathcal{G}$. This means that the left Cayley graph with adjacency matrix $\mathsf{PAP}^{\mathsf{T}}$ is isomorphic to $\mathscr{G}_{\mathrm{A}}$, as conjugation by h is a group automorphism on $\mathcal{G}$, and given a group automorphism $\sigma : \mathcal{G} \to \mathcal{G}$, we get a graph isomorphism $\mathrm{Cay}_{\mathrm{l}}(\mathcal{G}, \mathcal{A}) \cong \mathrm{Cay}_{\mathrm{l}}(\mathcal{G}, \sigma(\mathcal{A}))$. The graph $\mathscr{G}$ is labeled by $\mathcal{A} \sqcup \mathcal{A}$ in a natural way, where $(a, 0) \in \mathcal{A} \sqcup \mathcal{A}$ does group multiplication by a inside the first component and multiplication by hah^{-1} inside the second, and $(a, 1) \in \mathcal{A} \sqcup \mathcal{A}$ multiplies with a and swaps component.

This will be helpful to us because right Cayley graphs of $\mathcal{G}$ commute with left Cayley graphs of $\mathcal{G}$, in particular for the labeling sets $\mathcal{A}$ and $\sigma(\mathcal{A})$. We get a bound on the expansion λ of this graph from Proposition 7, and the following lemma gives a sufficient condition for our graph to be non-Cayley in the sense that the labeling on it is not the labeling of a Cayley graph.

Lemma 8. *The Schreier graph $\mathscr{G}$ described above is not a Cayley graph if there exists $a_i, a_j \in \mathcal{A}$ such that $a_j a_i h \neq h a_j a_i$.*

Proof: Starting at any vertex in the first component, it is clear that the path $(a_i, 0)^{-1}(a_j, 0)^{-1}(a_j, 1)(a_i, 1)$ is a loop. Starting at a vertex g in the second component, however, this path will have the endpoint $a_i^{-1} a_j^{-1} h^{-1} a_j a_i h g \neq g$. ∎

The problem of finding families of Ramanujan graphs where the degree is constant and the size grows arbitrarily large is considered hard, even though random graphs are believed to have a high probability of being Ramanujan. In our setting, we also need them to be commuting pairs of non-Cayley graphs. There is, however, a family of Ramanujan graphs due to Morgenstern [42], where the graphs are given as Cayley graphs of the projective special linear (PSL) group or projective general linear (PGL) group over a prime power order finite field. We fix a prime q, and consider Morgenstern's $(q+1)$-regular Cayley graphs for the powers of q.

Lemma 9. *If $\mathscr{G}_{\mathrm{A}} = \mathrm{Cay}_{\mathrm{l}}(\mathcal{G}, \mathcal{A})$ is one of the Ramanujan graphs due to Morgenstern, then there is an $h \in \mathcal{G}$ making the graph $\mathscr{G}$ described above non-Cayley.*

Proof: Fix $a_i, a_j \in \mathcal{A}$. Since the PSL and PGL groups are centerless, there is an $h \in \mathcal{G}$ such that $a_j a_i h \neq h a_j a_i$, and $\mathscr{G}$ constructed using this h is non-Cayley by Lemma 8. ∎

Remark 7. *Actually, there are many $h \in \mathcal{G}$ that would make $\mathscr{G}$ non-Cayley. For any h in a centerless group $\mathcal{G}$, there exists a $g \in \mathcal{G}$ not commuting with h. Since $\mathcal{A}$ generates $\mathcal{G}$, this g can be written as a product $g = a_{i_1} \dots a_{i_s}$ where $a_{i_t} \in \mathcal{A}$ for all $t \in [s]$. If it is possible to do this in such a way that s is even, then the product defines a path $(a_{i_s}^{-1}, 0) \dots (a_{i_1}^{-1}, 0)(a_{i_1}, 1) \dots (a_{i_s}, 1)$ that is a cycle when starting in one component, but not in the other.*

For each $i = 1, 2, \dots$ Lemma 9 gives a non-Cayley graph $\mathscr{G}$ of degree $2(q+1)$ made from the Ramanujan graph $\mathscr{G}_{\mathrm{A}} = \mathrm{Cay}_{\mathrm{l}}(\mathcal{G}, \mathcal{A})$ due to Morgenstern, where $\mathcal{G} = \mathrm{PGL}(2, q^i)$ or $\mathcal{G} = \mathrm{PSL}(2, q^i)$ (depending on a certain Legendre symbol), and Proposition 7 guaranties $\lambda(\mathscr{G}) \leq 4\sqrt{q}$. The graph $\mathscr{G}$ will commute with a graph that is two copies of $\mathrm{Cay}_{\mathrm{r}}(\mathcal{G}, \mathcal{B})$ for any $\mathcal{B} \subseteq \mathcal{G}$, and, recalling that left and right Cayley graphs are isomorphic, $\mathcal{B}$ can be picked such that $\lambda(\mathrm{Cay}_{\mathrm{r}}(\mathcal{G}, \mathcal{B})) \leq 2\sqrt{q}$. To make this graph $2(q+1)$-regular as well, we double the amount of edges by simply adding every edge one more time. The resulting graph has λ at most $4\sqrt{q}$. We let Δ be $2(q+1)$, the regularity of the graphs, and write $\mathscr{G}_{\mathrm{A}}$ for $\mathscr{G}$ and $\mathscr{G}_{\mathrm{B}}$ for the second graph. Now $\lambda(\mathscr{G}_{\mathrm{A}}) \leq \sqrt{2} \cdot 2\sqrt{\Delta - 1}$, and the same is true for the components of $\mathscr{G}_{\mathrm{B}}$. For readability we bound this by $\sqrt{2} \cdot 2\sqrt{\Delta}$.

We now turn to prove a bound on the minimum distance of codes constructed from the bipartite double covers of $\mathscr{G}_{\mathrm{A}}$ and $\mathscr{G}_{\mathrm{B}}$ using the quadripartite construction. Then, the vertex set $\mathcal{V}$ naturally splits into $\mathcal{V} = \mathcal{V}_{00} \sqcup \mathcal{V}_{01} \sqcup \mathcal{V}_{10} \sqcup \mathcal{V}_{11}$, where each $\mathcal{V}_{ij}$ is isomorphic to the vertex set of the original $\mathscr{G}_{\mathrm{A}}$ and $\mathscr{G}_{\mathrm{B}}$. Using the shorthands $\bar{\imath} = 1 - i$ and $\bar{\jmath} = 1 - j$, edges from $\mathscr{G}_{\mathrm{A}}$ go between $\mathcal{V}_{ij}$ and $\mathcal{V}_{i\bar{\jmath}}$, while edges from $\mathscr{G}_{\mathrm{B}}$ go between $\mathcal{V}_{ij}$ and $\mathcal{V}_{\bar{\imath}j}$. We closely follow the proof from [28] to show that it still works on the graphs we use and to see how the bound changes for our family of graphs.

Let $\mathscr{C}_{\mathrm{A}}$ and $\mathscr{C}_{\mathrm{B}}$ be linear codes with parameters $[\Delta, k_{\mathrm{A}}, d_{\mathrm{A}}]$ and $[\Delta, k_{\mathrm{B}}, d_{\mathrm{B}}]$, respectively, where $\Delta = k_{\mathrm{A}} + k_{\mathrm{B}}$. Let δ be a bound on the relative minimum distance of the codes and their duals, so that $d_{\mathrm{A}}, d_{\mathrm{B}} \geq \delta\Delta$ and the same holds for the dual codes.

Definition 11. *The dual tensor code $(\mathscr{C}_{\mathrm{A}}^{\perp} \otimes \mathscr{C}_{\mathrm{B}}^{\perp})^{\perp} = \mathscr{C}_{\mathrm{A}} \otimes \mathbb{F}_2^{\Delta} + \mathbb{F}_2^{\Delta} \otimes \mathscr{C}_{\mathrm{B}}$ is κ-product-expanding if any codeword $\boldsymbol{x}$ can be written as $\boldsymbol{x} = \boldsymbol{c} + \boldsymbol{r}$ with $\boldsymbol{c} \in \mathscr{C}_{\mathrm{A}} \otimes \mathbb{F}_2^{\Delta}$ and $\boldsymbol{r} \in \mathbb{F}_2^{\Delta} \otimes \mathscr{C}_{\mathrm{B}}$ such that*

$$|\boldsymbol{x}| \geq \kappa\Delta(||\boldsymbol{c}||_{\mathrm{c}} + ||\boldsymbol{r}||_{\mathrm{r}}),$$

where $||\boldsymbol{c}||_{\mathrm{c}}$ and $||\boldsymbol{r}||_{\mathrm{r}}$ denote, respectively, the number of columns involved in the support of $\boldsymbol{c}$ and the number of rows involved in the support of $\boldsymbol{r}$.[6]

Product expansion was studied in [43], where it was shown that random dual tensor product codes are κ-product-

[6]Even though $\boldsymbol{x}$, $\boldsymbol{c}$, and $\boldsymbol{r}$ are matrices corresponding to a local view, we mostly view these as vectors in a Tanner code, slightly abusing our notation convention (i.e., vectors are denoted by bold letters, while matrices are denoted by sans serif uppercase letters). However, the difference should be clear from the context.

expanding for a constant κ with high probability as $\Delta \to \infty$, where κ only depends on the rates of the codes.

Throughout the rest of the section, $\boldsymbol{x}$ will be a codeword of our CSS code such that $\boldsymbol{x} \in \mathscr{C}_1$ and $\boldsymbol{x} \notin \mathscr{C}_0^\perp$. We will bound the Hamming weight of $\boldsymbol{x}$ from below, assuming that the local codes used are κ-product-expanding dual tensor codes.

Recall that the entries of $\boldsymbol{x}$ are associated with edges of the bipartite Δ^2-regular graph $\mathscr{G}_1^\square$ with n edges. We will write $\mathcal{V}_1 = \mathcal{V}_{01} \cup \mathcal{V}_{10}$ for the vertices of this graph. To apply product expansion later, we choose a decomposition $\boldsymbol{x}_v = \boldsymbol{c}_v + \boldsymbol{r}_v$ of our codeword in the local code for every vertex $v \in \mathcal{V}_1$, where $\boldsymbol{c}_v$ and $\boldsymbol{r}_v$ both can be seen as $\Delta \times \Delta$-matrices (embedded in $\mathbb{F}_2^n$), the first with columns in $\mathscr{C}_\mathrm{A}$ and the second with rows in $\mathscr{C}_\mathrm{B}$. Let $\boldsymbol{C}_i \triangleq \sum_{v \in \mathcal{V}_{i\bar{\imath}}} \boldsymbol{c}_v$ and $\boldsymbol{R}_i \triangleq \sum_{v \in \mathcal{V}_{i\bar{\imath}}} \boldsymbol{r}_v$ and also $||\boldsymbol{C}_i||_\mathrm{C} \triangleq \sum_{v \in \mathcal{V}_{i\bar{\imath}}} ||\boldsymbol{c}_v||_\mathrm{c}$ and $||\boldsymbol{R}_i||_\mathrm{R} \triangleq \sum_{v \in \mathcal{V}_{i\bar{\imath}}} ||\boldsymbol{r}_v||_\mathrm{r}$. Note that these sums are disjoint in the sense that for example $\boldsymbol{C}_0$ restricted to some $v \in \mathcal{V}_{10}$ is $\boldsymbol{c}_v$. Now $\boldsymbol{x} = \boldsymbol{C}_0 + \boldsymbol{R}_1 = \boldsymbol{C}_1 + \boldsymbol{R}_0$, and we may assume that our chosen decomposition minimizes $||\boldsymbol{x}|| \triangleq ||\boldsymbol{C}_0||_\mathrm{C} + ||\boldsymbol{R}_0||_\mathrm{R} + ||\boldsymbol{C}_1||_\mathrm{C} + ||\boldsymbol{R}_1||_\mathrm{R}$, called the *norm* of $\boldsymbol{x}$.

We may furthermore assume that our chosen decomposition of $\boldsymbol{x}$ is also a minimal representation for $\boldsymbol{x}^0 \triangleq \boldsymbol{C}_0 + \boldsymbol{R}_0 = \boldsymbol{C}_1 + \boldsymbol{R}_1$, a codeword in the Tanner code on $\mathscr{G}_0^\square$, in terms of $||\boldsymbol{x}^0||$, see Lemma 7 of [28]. There is an induced decomposition $\boldsymbol{x}_w = \boldsymbol{c}_w + \boldsymbol{r}_w$ for $w \in \mathcal{V}_{ii}$ since $\mathcal{E}^{\mathcal{Q}}(w)$ shares exactly Δ columns with the set of local views $\mathcal{E}^{\mathcal{Q}}(v)$ for $v \in \mathcal{V}_{i\bar{\imath}}$, and similarly also Δ rows for $v \in \mathcal{V}_{i\bar{\imath}}$. This lets us consider $\boldsymbol{c}_v$ and $\boldsymbol{r}_v$ for any vertex of $\mathcal{X}$.

Let $\mathcal{S}_{ij}$ be the set of vertices $v \in \mathcal{V}_{ij}$ where $\boldsymbol{c}_v + \boldsymbol{r}_v$ (that is, $\boldsymbol{C}_j + \boldsymbol{R}_i$ restricted to $\mathcal{E}^{\mathcal{Q}}(v)$) is nonzero. Recall that $\boldsymbol{C}_j + \boldsymbol{R}_i$ is $\boldsymbol{x}$ when $i \neq j$ and $\boldsymbol{x}^0$ when $i = j$. We will also write $\mathcal{S}_0$ for $\mathcal{S}_{00} \cup \mathcal{S}_{11}$, and $\mathcal{S}_1$ for $\mathcal{S}_{01} \cup \mathcal{S}_{10}$. Let the *exceptional vertices* be the $v \in \mathcal{V}$ where $||\boldsymbol{c}_v||_\mathrm{c} + ||\boldsymbol{r}_v||_\mathrm{r} \geq \frac{1}{2}\alpha\Delta$ with $\alpha = \delta^2/256$. We write $\mathcal{S}_{ij}^\mathrm{e}$ for the exceptional vertices in $\mathcal{S}_{ij}$, and call the vertices of $\mathcal{S}_{ij}$ that are not exceptional *ordinary*.

The following is analog to Lemma 10 in [28].

Lemma 10. *If* $|\mathcal{S}_{ij}| \leq \frac{1}{2}\frac{\alpha\kappa}{2}|\mathcal{V}_{00}|$, *then*

$$|\mathcal{S}_{i\bar{\imath}}^\mathrm{e}| \leq \frac{256}{(\frac{1}{2}\alpha)^2\kappa^2\Delta^2}|\mathcal{S}_0| \quad \textit{and} \quad |\mathcal{S}_{i\bar{\imath}}^\mathrm{e}| \leq \frac{256}{(\frac{1}{2}\alpha)^2\kappa^2\Delta^2}|\mathcal{S}_1|.$$

Proof: Appendix A-D in the supplementary material. ∎

Recall that given $i, j \in \{0, 1\}$, the local view $\mathcal{E}^{\mathcal{Q}}(v)$ of a vertex $v \in \mathcal{V}_{ij}$ shares in total Δ columns with local views of vertices of $\mathcal{V}_{\bar{\imath}j}$. We let $\mathcal{T} \subseteq \mathcal{V}_{ij}$ be the set consisting of vertices $v \in \mathcal{V}_{ij}$ such that $\boldsymbol{c}_v$ contains a nonzero column where the vertex $w \in \mathcal{V}_{\bar{\imath}j}$ such that $\mathcal{E}^{\mathcal{Q}}(w)$ shares the column is ordinary. The following is analog to Lemma 11 of [28].

Lemma 11. *If* $|\mathcal{S}_{i\bar{\jmath}}| \leq \delta|\mathcal{V}_{00}|/8$, *then*

$$|\mathcal{T}| \leq \frac{2 \cdot 64}{\delta^2\Delta}|\mathcal{S}_{i\bar{\jmath}}|.$$

The same holds when swapping columns for rows and $\mathcal{V}_{\bar{\imath}j}$ *for* $\mathcal{V}_{i\bar{\jmath}}$ *in the definition of* $\mathcal{T}$.

Proof: Appendix A-E in the supplementary material. ∎

The following is analog to Lemma 8 of [28].

Lemma 12. *For any* $\boldsymbol{x} \in \mathscr{C}_1 \setminus \mathscr{C}_0^\perp$, *we have* $||\boldsymbol{x}|| \geq \frac{1}{2}\frac{\delta^2\kappa n}{512\Delta^2}$.

Proof: Appendix A-F in the supplementary material. ∎

Theorem 3. *The minimum distance of the quantum Tanner code satisfies* $d \geq \frac{\delta^2\kappa^2 n}{2 \cdot 1024\Delta}$.

Proof: Appendix A-G in the supplementary material. ∎

Theorem 3 is analog to Theorem 9 of [28], where they obtain the bound $d \geq \frac{\delta^2\kappa^2 n}{1024\Delta}$.[7] The quality of the bound is sacrificed for readability to the same degree here as in [28]. The extra factor $\frac{1}{2}$ in our bound stems from the added factor $\sqrt{2}$ in the spectral expansions of $\mathscr{G}_\mathrm{A}$ and the components of $\mathscr{G}_\mathrm{B}$ in the family of graphs we consider. One should keep in mind that the best codes are in practice not likely to be the ones in this family. We consider a more promising method for concrete codes in the next section.

Proof of Theorem 2: Let $\rho \in (0, 1/2)$ and $\delta > 0$ satisfying $H_2(\delta) < \rho$ be given, where $H_2(x) = -x\log_2(x) - (1-x)\log_2(1-x)$ is the binary entropy function. Random codes of rate $1 - \rho$ are likely to have a relative minimum distance of at least δ for large enough lengths [45], so when $\mathscr{C}_\mathrm{A}, \mathscr{C}_\mathrm{B}$ are picked randomly with rates ρ and $1-\rho$, the codes $\mathscr{C}_\mathrm{A}, \mathscr{C}_\mathrm{A}^\perp, \mathscr{C}_\mathrm{B}, \mathscr{C}_\mathrm{B}^\perp$ are all likely to have a relative minimum distance at least δ. Corollary 1 of [43] says that for the given rates, there is a κ such that $(\mathscr{C}_\mathrm{A} \otimes \mathscr{C}_\mathrm{B})^\perp$ and $(\mathscr{C}_\mathrm{A}^\perp \otimes \mathscr{C}_\mathrm{B}^\perp)^\perp$ are both κ-product-expanding with high probability for large enough Δ. Theorem 3 says that our family of graphs achieves the desired minimum distance when Δ is large enough. ∎

V. Numerical Results

In this section, we compare the performance of quantum Tanner codes based on connected Cayley graphs (i.e., codes from the original construction) and our proposed generalized quantum Tanner codes based on Schreier graphs, both in terms of minimum distance and simulated logical error rate on the depolarizing channel, under binary and quaternary BP decoding with ordered statistics decoding (OSD) post-processing as in [15].[8] To the best of our knowledge, this is the first simulation study on quantum Tanner codes. The Schreier graphs we construct here are not by construction guaranteed to be non-Cayley, but at least one of the two graphs going into the construction will have two components, and we are hence outside the original construction.

We propose searching for graphs with the best spectral expansion properties and construct codes from these optimal expanders. Doing this for both constructions using the same local codes, should lead to a fair comparison. For simplicity, only codes from the quadripartite construction are considered, meaning that we will force the condition of having no overlapping edges (equivalent to TNC in the Cayley case) to hold instead of searching for graphs where it holds. Furthermore, we will use the bipartite double cover to find common bipartitions. For codes constructed from Cayley graphs, this means searching through all groups $\mathcal{G}$ (of a given size) and

[7] There is a slight miscalculation in the proof of Theorem 9 of [28] leading to the constant $\frac{\delta^2\kappa^2}{256\Delta}$ instead of $\frac{\delta^2\kappa^2}{1024\Delta}$ [44].

[8] The binary BP decoding simulations are based on the implementation from [46], [47, Sec. IV-A], while the quaternary BP decoding part of our simulations is based on the implementation at https://github.com/kit-cel/Quantum-Neural-BP4-demo with the OSD part implemented in house.

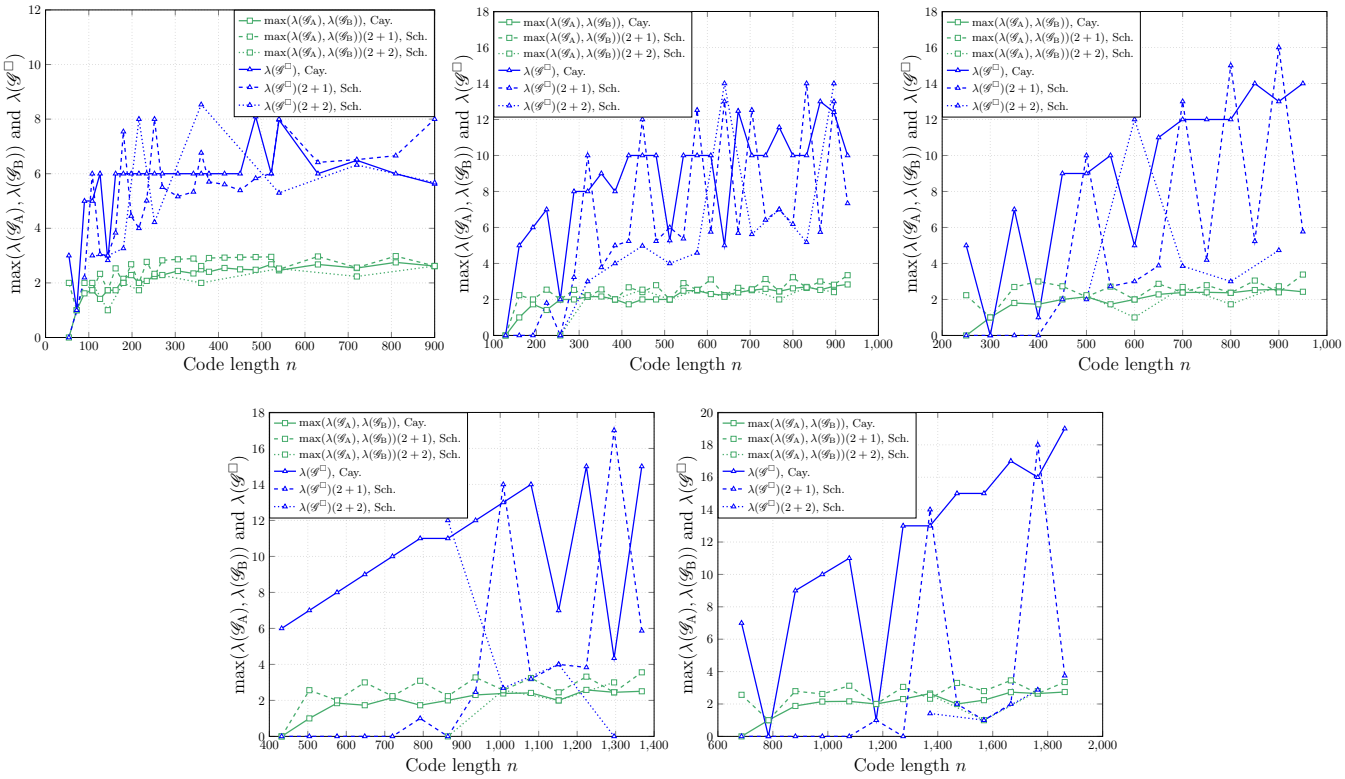

Fig. 4. Comparing the best spectral expansion properties of the Cayley and Schreier constructions for different values of the code length n, for $\Delta = 3, 4, 5, 6, 7$ (left to right, top to bottom). See paragraphs 2 to 6 of Section V for an explanation.

all corresponding self-inverse subsets $\mathcal{A} \subseteq \mathcal{G}$ and $\mathcal{B} \subseteq \mathcal{G}$, for a given value of Δ (the length of the local codes), giving an overall code length of $\Delta^2|\mathcal{G}|$ for the quantum Tanner code. We prioritize the expansion of $\mathscr{G}_\mathrm{A}$ and $\mathscr{G}_\mathrm{B}$ first, and then the expansion of $\mathscr{G}^\square$, where expansion is measured by λ of the connected components. Even though these expansions (seem to) have a positive impact on the minimum distance of the code, it should be noted that different graphs with the same expansions constructed from the same group can have different parameters, even if the same local codes are used, so when searching for good codes it is usually not enough to look at a single optimal graph. For generalized quantum Tanner codes, the search (which is not the most general search one can do) is more elaborate and is conducted as follows.

For a given group order and length of local code Δ, we consider the groups $\mathcal{G}$ of this order and subsets $\mathcal{A}_1, \mathcal{A}_2, \mathcal{A}_3 \subseteq \mathcal{G}$ such that $\mathcal{A}_1$ and $\mathcal{A}_3$ are symmetric, $|\mathcal{A}_1| = |\mathcal{A}_3|$, and $|\mathcal{A}_1| + |\mathcal{A}_2| = \Delta$. This defines a Δ-regular Schreier graph $\mathscr{G}'_\mathrm{A}$ consisting of the two Cayley graphs $\mathrm{Cay}_\mathrm{l}(\mathcal{G}, \mathcal{A}_1)$ and $\mathrm{Cay}_\mathrm{l}(\mathcal{G}, \mathcal{A}_3)$ connected by the bipartite double cover of $\mathrm{Cay}_\mathrm{l}(\mathcal{G}, \mathcal{A}_2)$, where elements $a \in \mathcal{A}_2$ can be considered self-inverse if desired. We consider splits $\Delta = |\mathcal{A}_1| + |\mathcal{A}_2|$ that are as fair as possible, i.e., $|\mathcal{A}_1| = |\mathcal{A}_2|$ or $|\mathcal{A}_1| = |\mathcal{A}_2| \pm 1$, and search for $\mathscr{G}'_\mathrm{A}$ with small $\lambda(\mathscr{G}'_\mathrm{A})$. We search for $\mathscr{G}'_\mathrm{B}$ in the same way using right Cayley graphs instead of left.

Then, we can either set $\mathscr{G}_\mathrm{A}$ equal to the quadripartite cover of $\mathscr{G}'_\mathrm{A}$ and $\mathscr{G}_\mathrm{B}$ equal to two copies of the quadripartite cover of a Cayley graph over the same group $\mathcal{G}$ to obtain a code of length $2\Delta^2|\mathcal{G}|$, or we can set $\mathscr{G}_\mathrm{A}$ and $\mathscr{G}_\mathrm{B}$ equal to two copies of the quadripartite covers of $\mathscr{G}'_\mathrm{A}$ and $\mathscr{G}'_\mathrm{B}$, respectively, to obtain codes of length $4\Delta^2|\mathcal{G}|$. We denote the first case $(2+1)$ and the second $(2+2)$. In the second case, $\mathrm{Cay}_\mathrm{l}(\mathcal{G}, \mathcal{A}_2)$ in one component of $\mathscr{G}_\mathrm{A}$ should connect the two copies of $\mathrm{Cay}_\mathrm{r}(\mathcal{G}, \mathcal{B}_1)$, and in the other component it should connect the two copies of $\mathrm{Cay}_\mathrm{r}(\mathcal{G}, \mathcal{B}_3)$. The same should hold when swapping the roles of $\mathcal{A}$ and $\mathcal{B}$.

Fix some ordering on $\mathcal{G}$ and let $\mathsf{A}_i, \mathsf{B}_j$ be the adjacency matrices of the above-mentioned Cayley graphs for the sets $\mathcal{A}_i$, $\mathcal{B}_j$ for the given ordering on $\mathcal{G}$. In the case where $n = 2\Delta^2|\mathcal{G}|$, the graphs $\mathscr{G}_\mathrm{A}$ and $\mathscr{G}_\mathrm{B}$ will have adjacency matrices $\left[\begin{array}{c|c} \mathsf{A}_1 & \mathsf{A}_2 \\ \hline \mathsf{A}_2^\mathsf{T} & \mathsf{A}_3 \end{array}\right]$ and $\left[\begin{array}{c|c} \mathsf{B} & 0 \\ \hline 0 & \mathsf{B} \end{array}\right]$, where B is the adjacency matrix of a connected Cayley graph of $\mathcal{G}$. In the other case where $n = 4\Delta^2|\mathcal{G}|$, the graphs $\mathscr{G}_\mathrm{A}$ and $\mathscr{G}_\mathrm{B}$ will have adjacency matrices

$$\begin{bmatrix} \mathsf{A}_1 & 0 & \mathsf{A}_2 & 0 \\ 0 & \mathsf{A}_1 & 0 & \mathsf{A}_2 \\ \mathsf{A}_2^\mathsf{T} & 0 & \mathsf{A}_3 & 0 \\ 0 & \mathsf{A}_2^\mathsf{T} & 0 & \mathsf{A}_3 \end{bmatrix} \quad \text{and} \quad \begin{bmatrix} \mathsf{B}_1 & \mathsf{B}_2 & 0 & 0 \\ \mathsf{B}_2^\mathsf{T} & \mathsf{B}_3 & 0 & 0 \\ 0 & 0 & \mathsf{B}_1 & \mathsf{B}_2 \\ 0 & 0 & \mathsf{B}_2^\mathsf{T} & \mathsf{B}_3 \end{bmatrix}.$$

We first search for the best expansion among the possible $\mathscr{G}_\mathrm{A}$ and $\mathscr{G}_\mathrm{B}$. From these, we can construct codes of length $4\Delta^2|\mathcal{G}|$. We also see which groups give good expansion for both Schreier and Cayley graphs, and then we can construct codes of length $2\Delta^2|\mathcal{G}|$ from these. Among the graphs with optimal expansion, priority is given to the ones with a low $\lambda(\mathscr{G}^\square)$. There is often some variation among the performance of codes from graphs with the same expansions. Hence, we consider multiple instances for each code length and rate.

In Fig. 4, we show the best spectral expansions $\max(\lambda(\mathscr{G}_\mathrm{A}), \lambda(\mathscr{G}_\mathrm{B}))$ (green curves) and $\lambda(\mathscr{G}^\square)$ (blue curves) for different values of the block length n for $\Delta = 3, 4, 5, 6, 7$ (left to right, top to bottom). The pairs consisting of a Cayley

TABLE I
LIST OF (GENERALIZED) QUANTUM TANNER CODES[a]

Code	$[[n,k,d]]$	$\mathcal{G}$	$\lvert\mathcal{G}\rvert$	$\mathcal{A}$	$\mathcal{B}$	$\mathscr{C}_\mathrm{A}$	$\mathscr{C}_\mathrm{B}$	Δ	$\lambda(\mathscr{G}_\mathrm{A})$	$\lambda(\mathscr{G}_\mathrm{B})$	$\lambda(\mathscr{G}^{\square})$	w_r	weight range
$\mathscr{C}_{180}^{\mathrm{Cay}}$	$[[180,28,5]]$	$\mathcal{D}_{10}$	20	$\{r^7s, r^4s, r^6s\}$	$\{r^3s, r^4s, s\}$	$\mathscr{C}_\mathrm{Rep}$	$\mathscr{C}_\mathrm{SPC}$	3	2.15	2.15	6	6	6
$\mathscr{C}_{180}^{\mathrm{Sch}}$	$[[180,26,6]]$	$\mathcal{Z}_5$	5	$\{g,g^4\},\{1\},\{g^2,g^3\}$	$\{g,g^4\},\{1\},\{g^2,g^3\}$	$\mathscr{C}_\mathrm{Rep}$	$\mathscr{C}_\mathrm{SPC}$	3	2	2	3.26	6	6
$\mathscr{C}_{500}^{\mathrm{OOLM}}$	$[[500,42,4]]$	$\mathcal{G}_\mathrm{OOLM}$	20	$\{1,s,s^3,t^2,s^2,t^3s^2\}$	$\{1,ts^3,t^2s,t^2s^2,t^4s^2\}$	$\mathscr{C}_\mathrm{a}$	$\mathscr{C}_\mathrm{b}$	5	2.79	2.79	3.42	8.1	6–12
$\mathscr{C}_{500}^{\mathrm{Sch}}$	$[[500,42,6]]$	$\mathcal{Z}_5$	5	$\{g,g^4\},\{1,g,g^4\},\{g^2,g^3\}$	$\{g^2,g^3\},\{1,g^2,g^3\},\{g,g^4\}$	$\mathscr{C}_\mathrm{a}$	$\mathscr{C}_\mathrm{b}$	5	2.24	2.24	2	8.1	6–12
$\mathscr{C}_{500}^{\mathrm{Cay}}$	$[[500,46,6]]$	$\mathcal{D}_{10}$	20	$\{s,r^6s,r^8s,r^5s,r^9s\}$	$\{s,r^8s,r^5s,rs,r^9s\}$	$\mathscr{C}_\mathrm{a}$	$\mathscr{C}_\mathrm{b}$	5	2.15	2.15	9	8.1	6–12
$\mathscr{C}_{686}^{\mathrm{Cay}}$	$[[686,34,13]]$	$\mathcal{D}_7$	14	$\{s,rs,r^2s,r^3s,r^4s,r^5s,r^6s\}$	$\{1,s,r^2s,r,r^6,r^3,r^4\}$	$\mathscr{C}_\mathrm{c}$	$\mathscr{C}_\mathrm{d}$	7	0	3.05	0	13	12–16
$\mathscr{C}_{686}^{\mathrm{Sch}}$	$[[686,28,14]]$	$\mathcal{Z}_7$	7	$\{g^2g^5g^3g^4\}\{1,g,g^4\}$ $\{g,g^6,g^3,g^4\}$	$\{1,g,g^6,g^2,g^5,g^3,g^4\}$	$\mathscr{C}_\mathrm{c}$	$\mathscr{C}_\mathrm{d}$	7	2.57	0	0	13	12–16

[a]Here, $\mathscr{C}_\mathrm{Rep}$, $\mathscr{C}_\mathrm{SPC}$, $\mathscr{C}_\mathrm{a}$, $\mathscr{C}_\mathrm{b}$, $\mathscr{C}_\mathrm{c}$, and $\mathscr{C}_\mathrm{d}$, are the linear codes with parity-check matrices $\left[\begin{smallmatrix}1&0&1\\0&1&1\end{smallmatrix}\right]$, $[1\,1\,1]$, $\left[\begin{smallmatrix}1&1&1&0&0&0\\0&0&1&1&1&1\end{smallmatrix}\right]$, $\left[\begin{smallmatrix}1&1&1&0&0\\0&1&1&1&0\\0&0&1&1&1\end{smallmatrix}\right]$, $\left[\begin{smallmatrix}1&0&1&1&1&0&0\\0&1&1&1&0&1&0\\0&0&0&1&1&1&1\end{smallmatrix}\right]$, and $\left[\begin{smallmatrix}1&0&0&1&0&1&1\\0&1&0&1&0&1&0\\0&0&1&1&0&0&1\\0&0&0&0&1&1&1\end{smallmatrix}\right]$, respectively. $\mathcal{D}_m$ is the dihedral group of order $2m$, and $\mathcal{G}_\mathrm{OOLM}$ is the group generated by s,t with relations $s^4=t^5=1, ts=st^2$, considered in [14]. The average row weight of the parity-check matrices used for decoding is denoted by w_r, while the last column shows the corresponding weight range. See Appendix B for the construction of parity-check matrices.

TABLE II
LIST OF GENERALIZED BICYCLE CODES[b]

Code	$[[n,k,d]]$	ℓ	$a(x)$	$b(x)$	w_r
$\mathscr{C}_{180}^{\mathrm{GB}}$	$[[180,26,7]]$	90	$1+x^{19}+x^{81}+x^{82}$	$1+x^{59}+x^{68}+x^{72}$	8
$\mathscr{C}_{480}^{\mathrm{GB}}$	$[[480,40,12]]$	240	$1+x^{76}+x^{100}+x^{143}+x^{216}+x^{223}$	$1+x^{32}+x^{57}+x^{77}+x^{117}+x^{225}$	12
$\mathscr{C}_{688}^{\mathrm{GB}}$	$[[688,30,\geq 19]]$	344	$1+x^{17}+x^{77}+x^{97}+x^{125}+x^{145}+x^{146}+x^{265}$	$1+x^4+x^{116}+x^{120}+x^{196}+x^{207}+x^{214}+x^{282}$	16

[b]Here, the polynomials $a(x)$ and $b(x)$ uniquely describe the code as outlined in [15, Sec. 4]. w_r is the constant parity-check matrix row weight.

graph of two components and a connected Schreier graph $(2+1)$ are dashed, the pairs consisting of two-component Schreier graphs $(2+2)$ are dotted, and the solid curves correspond to connected Cayley graphs. For Cayley graphs, the search is exhaustive, while for Schreier graphs, we sampled randomly. We remark that $\lambda(\mathscr{G}_\mathrm{A}) = \lambda(\mathscr{G}_\mathrm{B})$ for the dotted and the solid curve, while for the dashed they are often not. As can be seen from the figure, the Schreier construction outperforms the Cayley construction for $\lambda(\mathscr{G}^{\square})$ (the minimum of the blue dashed and dotted curves is in general lower than the blue solid curve), while for $\max(\lambda(\mathscr{G}_\mathrm{A}),\lambda(\mathscr{G}_\mathrm{B}))$ we generally observe the opposite behavior (the green solid curve is in many cases lower than the minimum of the green dashed and dotted curves). We will see that codes from the dotted and dashed lines can outperform those from the solid in cases where $\max(\lambda(\mathscr{G}_\mathrm{A}),\lambda(\mathscr{G}_\mathrm{B}))$ is smaller or similar to the former.

Based on the search procedure outlined above, we constructed several codes of length 180, 500, and 686, and tested their performance on the depolarizing channel under quaternary BP decoding (with a maximum of 6 iterations) and with OSD post-processing of order 1. The parity-check matrices we used are constructed as described in Appendix B in the supplementary material. We note that they all have some redundant checks and perform worse when these are removed, which is consistent with the results from [18]. In fact, we observed a larger loss for codes from the Cayley construction than from the Schreier one. For code length 180 and for the Cayley construction, we used a group size of 20 and $\Delta = 3$. There are 5 non-equivalent groups of size 20, and we tested several codes (with the best expansion properties) based on four of these groups (the fifth group gives no connected Cayley graphs for $\Delta = 3$, so we did not construct any codes based on this group). Their performance is depicted in Fig. 5 (left-most plot), where curves of different colors (blue, green, magenta, and yellow) correspond to different groups. As can be seen from the plot, the performance clusters into several clusters. The expansion of the input Cayley graphs correctly predicts which groups give the best clusters. The codes corresponding to the blue curves in this plot are all from the dihedral group $\mathcal{D}_{10}$ or order 10, while the other groups (green, yellow, magenta) perform worse. From this experiment, we identified one of the best performing quantum codes (from the lower cluster of blue curves), denoted by $\mathscr{C}_{180}^{\mathrm{Cay}}$. Its parameters are given in Table I (first row). Next, we did the same for both the $(2+1)$ and $(2+2)$ Schreier construction, resulting in the upper and lower orange curves, respectively. We picked one of the best performing codes, denoted by $\mathscr{C}_{180}^{\mathrm{Sch}}$, and give its parameters in the second row of Table I. As can be seen from the plot, $\mathscr{C}_{180}^{\mathrm{Sch}}$ outperforms all of the simulated codes based on the Cayley construction, which we believe can be attributed to an improved minimum distance (see Table I).

For comparison, we also constructed several random generalized bicycle (GB) codes that generally perform well in the finite-length regime, and are believed to give large minimum distance, by following the approach proposed in [15, Sec. 4]. This approach is able to obtain an *ansatz* of well-performing code families with similar lengths and rates as those chosen in our simulation study. The GB codes have code parameters $[[n,k]] = [[2\ell,k]]$ for some $\ell \in \mathbb{N}$. We identified GB codes with code parameters that are closest to the code instances from the Schreier and Cayley constructions. The simulated performance of these codes (again with redundant parity-check matrices) is depicted by the brown curves, and one of the best-performing codes is listed in Table II (first row).

For code lengths 500 and 686, we repeated the same exercise as for length 180. For length 686, only one pair of

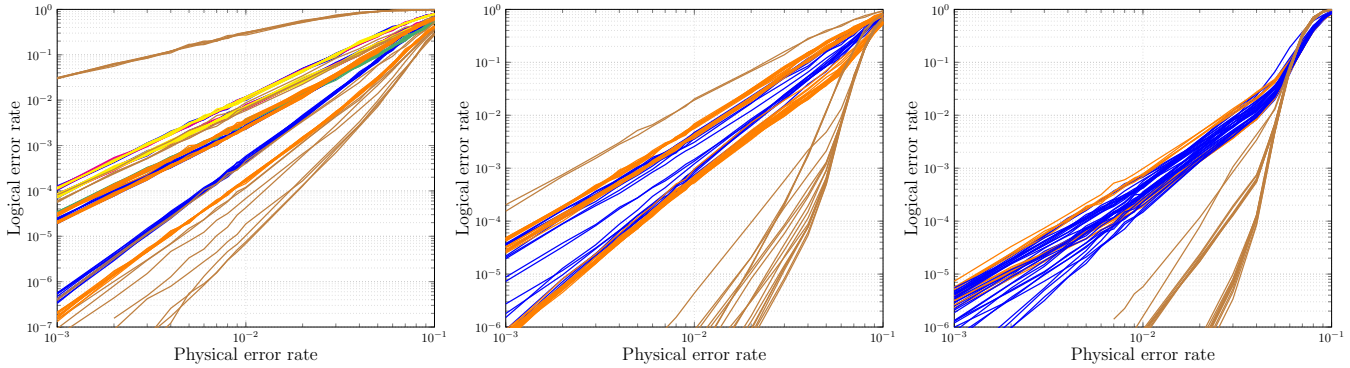

Fig. 5. Comparing the logical error rate performance of (generalized) quantum Tanner codes based on Schreier and Cayley graphs and GB codes on the depolarizing channel under quaternary BP decoding with OSD post-processing of order 1. Left plot: $n = 180$, middle plot: $n = 500$ (480 for the GB codes), and right plot: $n = 686$ (688 for the GB codes). Orange: based on Schreier graphs, brown: GB codes, remaining colors: based on Cayley graphs.

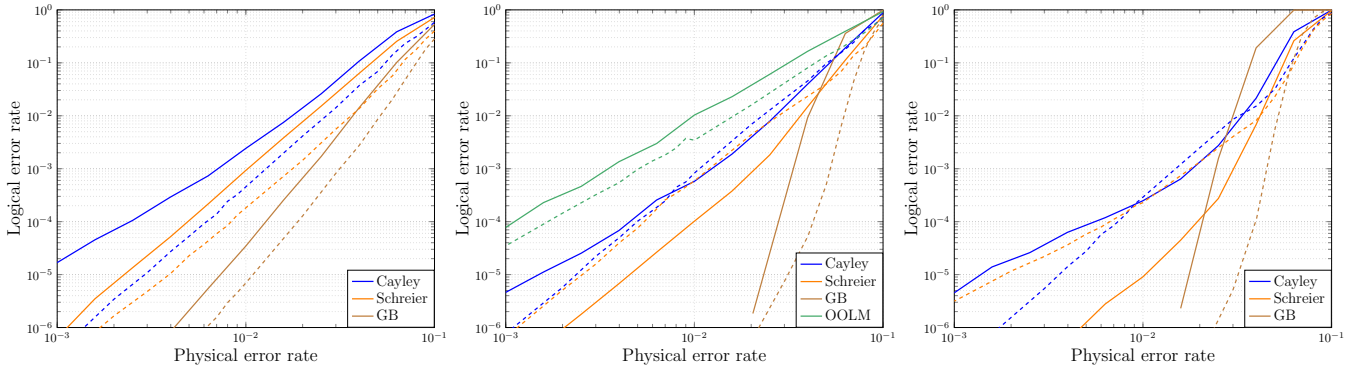

Fig. 6. Comparing the logical error rate performance of (generalized) quantum Tanner codes based on Schreier and Cayley graphs and GB codes on the depolarizing channel. Left plot: $n = 180$, middle plot: $n = 500$ (480 for the GB code), and right plot: $n = 686$ (688 for the GB code). Dashed curves are for quaternary BP decoding with OSD post-processing of order 1, while solid curves are for binary BP decoding with OSD-CS-7 post-processing.

Cayley graphs had the optimal $\lambda(\mathcal{G}_A) = \lambda(\mathcal{G}_B) = 0$, so we enlarged the search space a bit. Also, no $(2+2)$ codes could be constructed. For $n = 500$, the best performing code from the Schreier construction (orange curves, middle plot of Fig. 5) outperforms the best code from the Cayley construction (blue curves), while for $n = 686$, we see the opposite behavior (same colors, right-most plot). Some of the best performing corresponding codes and their parameters are listed in Table I. As for $n = 180$, we also compare with randomly constructed GB codes of comparable lengths and rates (brown curves), and some of the best performing corresponding codes are listed in Table II.

The minimum distance of the codes in Tables I and II is calculated using the classical algorithm in [48], [49]. In particular, an exhaustive list of all nonzero codewords of weight at most τ (for some small value of τ) of $\mathscr{C}_0$ and $\mathscr{C}_1$ is first found using the algorithm in [48], [49]. Then, these two lists are filtered based on $\mathscr{C}_1^\perp$ and $\mathscr{C}_0^\perp$, respectively, i.e., if a codeword belongs to the row space of H_1 and H_0, respectively, it is filtered out. If there are still codewords left in the lists after filtering, then the minimum distance of the quantum code will be the minimum weight of these codewords. Otherwise, we increase τ by 1 and iterate the procedure.

In Fig. 6, we show the performance of the codes from Tables I and II under both quaternary BP decoding (with OSD post-processing of order 1 and a maximum of 6 BP iterations; dashed curves) and binary BP decoding (with OSD-CS-7 post-processing and a maximum of 1000 BP iterations; solid curves). In addition to codes among the best in Fig. 5, we have also added $\mathscr{C}_{500}^{\text{OOLM}}$ (green, middle plot), a quantum Tanner code constructed from the pair of Cayley graphs considered in [14]. This code, however, performs worse than the codes we obtained from our search. Interestingly, for $n = 500$ and $n = 686$, binary BP decoding significantly outperforms quaternary BP decoding for the Schreier code, while the opposite behavior is observed for the Cayley code. For $n = 180$ (for both the Cayley and the Schreier code) and for GB codes (for all three lengths), quaternary BP decoding performs the best. However, for all three lengths the Schreier code (under the best decoder) outperforms the corresponding Cayley code, while there is some performance loss compared to the best GB code. Quantum Tanner codes and our generalized version are, however, still useful, as they are asymptotically good. Note that the average check weight w_r, as well as much of the weight range, is higher than the minimum distance for most of the codes we have considered here, see Tables I and II.

VI. Conclusion and Future Work

We have generalized the construction of quantum Tanner codes from Cayley graphs to graphs with labeled local views and characterized it in several ways. Then, we showed that the construction contains asymptotically good quantum LDPC

codes that are not contained in the original construction. Finally, we evaluated the constructed codes' performance by measuring their logical error rate on the depolarizing channel and their minimum distance, showing that our proposed codes outperform the ones based on Cayley graphs. We conclude that it is worthwhile not to limit oneself to left-right Cayley complexes when considering quantum Tanner codes.

For future work, it would be interesting to try to construct codes that compete with the current state-of-the-art (e.g., the codes from [13]), compare them with finite-length codes from the construction presented in [8], and see how theoretical decoders specific for the construction behave in practice, possibly for a circuit-based noise model. The connection to the broader family of sheaf codes [38] could also be investigated, potentially giving rise to new promising constructions.

REFERENCES

[1] O. Å. Mostad, E. Rosnes, and H.-Y. Lin, "Generalizing quantum Tanner codes," in *Proc. IEEE Int. Symp. Inf. Theory Workshops (ISIT-W)*, Athens, Greece, Jul. 7, 2024, pp. 1–6.

[2] P. W. Shor, "Scheme for reducing decoherence in quantum computer memory," *Phys. Rev. A*, vol. 52, no. 4, pp. R2493–R2496, Oct. 1995.

[3] A. Steane, "Multiple-particle interference and quantum error correction," *Proc. Roy. Soc. Lond. A*, vol. 452, no. 1954, pp. 2551–2577, Nov. 1996.

[4] A. R. Calderbank and P. W. Shor, "Good quantum error-correcting codes exist," *Phys. Rev. A*, vol. 54, no. 2, pp. 1098–1105, Aug. 1996.

[5] A. M. Steane, "Error correcting codes in quantum theory," *Phys. Rev. Lett.*, vol. 77, no. 5, pp. 793–797, Jul. 1996.

[6] D. Gottesman, "Class of quantum error-correcting codes saturating the quantum Hamming bound," *Phys. Rev. A*, vol. 54, no. 3, pp. 1862–1868, Sep. 1996.

[7] A. R. Calderbank, E. M. Rains, P. W. Shor, and N. J. A. Sloane, "Quantum error correction via codes over GF(4)," *IEEE Trans. Inf. Theory*, vol. 44, no. 4, pp. 1369–1387, Jul. 1998.

[8] P. Panteleev and G. Kalachev, "Asymptotically good quantum and locally testable classical LDPC codes," in *Proc. 54th Annu. ACM Symp. Theory Comput. (STOC)*, Rome, Italy, Jun. 20–24, 2022, pp. 375–388.

[9] A. Leverrier and G. Zémor, "Quantum Tanner codes," in *Proc. 63rd Annu. IEEE Symp. Found. Comput. Sci. (FOCS)*, Denver, CO, USA, Oct. 31–Nov. 03, 2022, pp. 872–883.

[10] I. Dinur, S. Evra, R. Livne, A. Lubotzky, and S. Mozes, "Locally testable codes with constant rate, distance, and locality," in *Proc. 54th Annu. ACM Symp. Theory Comput. (STOC)*, Rome, Italy, Jun. 20–24, 2022, pp. 357–374.

[11] N. P. Breuckmann and J. N. Eberhardt, "Balanced product quantum codes," *IEEE Trans. Inf. Theory*, vol. 67, no. 10, pp. 6653–6674, Oct. 2021.

[12] F. Arute *et al.*, "Quantum supremacy using a programmable superconducting processor," *Nature*, vol. 574, no. 7779, pp. 505–510, Oct. 2019.

[13] S. Bravyi, A. W. Cross, J. M. Gambetta, D. Maslov, P. Rall, and T. J. Yoder, "High-threshold and low-overhead fault-tolerant quantum memory," *Nature*, vol. 627, no. 8005, pp. 778–782, Mar. 2024.

[14] D. Ostrev, D. Orsucci, F. Lázaro, and B. Matuz, "Classical product code constructions for quantum Calderbank-Shor-Steane codes," *Quantum*, vol. 8, Jul. 2024, Art. no. 1420.

[15] P. Panteleev and G. Kalachev, "Degenerate quantum LDPC codes with good finite length performance," *Quantum*, vol. 5, Nov. 2021, Art. no. 585.

[16] V. Guemard and G. Zémor, "Moderate-length lifted quantum Tanner codes," Feb. 2025, arXiv:2502.20297v1 [quant-ph].

[17] H. Yao, W. A. Laban, C. Häger, A. Graell i Amat, and H. D. Pfister, "Belief propagation decoding of quantum LDPC codes with guided decimation," in *Proc. IEEE Int. Symp. Inf. Theory (ISIT)*, Athens, Greece, Jul. 7–12, 2024, pp. 2478–2483.

[18] S. Miao, A. Schnerring, H. Li, and L. Schmalen, "Quaternary neural belief propagation decoding of quantum LDPC codes with overcomplete check matrices," *IEEE Access*, vol. 13, pp. 25 637–25 649, 2025.

[19] K.-Y. Kuo and C.-Y. Lai, "Exploiting degeneracy in belief propagation decoding of quantum codes," *npj Quantum Inf.*, vol. 8, no. 111, pp. 1–9, Sep. 2022.

[20] E. Dennis, A. Kitaev, A. Landahl, and J. Preskill, "Topological quantum memory," *J. Math. Phys.*, vol. 43, no. 9, pp. 4452–4505, Sep. 2002.

[21] M. H. Freedman and D. A. Meyer, "Projective plane and planar quantum codes," *Found. Comput. Math.*, vol. 1, no. 3, pp. 325–332, Jul. 2001.

[22] H. Bombin and M. A. Martin-Delgado, "Topological quantum distillation," *Phys. Rev. Lett.*, vol. 97, no. 18, Oct. 2006, Art. no. 180501.

[23] D. S. Wang, A. G. Fowler, and L. C. L. Hollenberg, "Surface code quantum computing with error rates over 1%," *Phys. Rev. A*, vol. 83, no. 2, Feb. 2011, Art. no. 020302.

[24] J.-P. Tillich and G. Zémor, "Quantum LDPC codes with positive rate and minimum distance proportional to the square root of the blocklength," *IEEE Trans. Inf. Theory*, vol. 60, no. 2, pp. 1193–1202, Feb. 2014.

[25] S. Bravyi and M. B. Hastings, "Homological product codes," in *Proc. 46th Annu. ACM Symp. Theory Comput. (STOC)*, New York, NY, USA, May 31–Jun. 3, 2014, pp. 273–282.

[26] A. A. Kovalev and L. P. Pryadko, "Improved quantum hypergraph-product LDPC codes," in *Proc. IEEE Int. Symp. Inf. Theory (ISIT)*, Cambridge, MA, USA, Jul. 1–6, 2012, pp. 348–352.

[27] N. P. Breuckmann and B. M. Terhal, "Constructions and noise threshold of hyperbolic surface codes," *IEEE Trans. Inf. Theory*, vol. 62, no. 6, pp. 3731–3744, Jun. 2016.

[28] A. Leverrier and G. Zémor, "Decoding quantum Tanner codes," *IEEE Trans. Inf. Theory*, vol. 69, no. 8, pp. 5100–5115, Aug. 2023.

[29] A. Leverrier and G. Zémor, "Efficient decoding up to a constant fraction of the code length for asymptotically good quantum codes," *ACM Trans. Algorithms*, May 2024.

[30] S. Gu, C. A. Pattison, and E. Tang, "An efficient decoder for a linear distance quantum LDPC code," in *Proc. 55th Annu. ACM Symp. Theory Comput. (STOC)*, Orlando, FL, USA, Jun. 20–23, 2023, pp. 919–932.

[31] I. Dinur, M.-H. Hsieh, T.-C. Lin, and T. Vidick, "Good quantum LDPC codes with linear time decoders," in *Proc. 55th Annu. ACM Symp. Theory Comput. (STOC)*, Orlando, FL, USA, Jun. 20–23, 2023, pp. 905–918.

[32] I. Dinur, T.-C. Lin, and T. Vidick, "Expansion of high-dimensional cubical complexes: with application to quantum locally testable codes," in *Proc. 65th Annu. IEEE Symp. Found. Comput. Sci. (FOCS)*, Chicago, IL, USA, Oct. 27–30, 2024, pp. 379–385.

[33] P. Cayley, "Desiderata and suggestions: No. 1. The theory of groups," *Amer. J. Math.*, vol. 1, no. 1, pp. 50–52, 1878.

[34] J. L. Gross, "Every connected regular graph of even degree is a Schreier coset graph," *J. Combinatorial Theory, Ser. B*, vol. 22, no. 3, pp. 227–232, Jun. 1977.

[35] A. Lubotzky, R. Phillips, and P. Sarnak, "Ramanujan graphs," *Combinatorica*, vol. 8, no. 3, pp. 261–277, Sep. 1988.

[36] S. Hoory, N. Linial, and A. Wigderson, "Expander graphs and their applications," *Bull. Amer. Math. Soc.*, vol. 43, no. 04, pp. 439–562, Aug. 2006.

[37] R. M. Tanner, "A recursive approach to low complexity codes," *IEEE Trans. Inf. Theory*, vol. 27, no. 5, pp. 533–547, Sep. 1981.

[38] P. Panteleev and G. Kalachev, "Maximally extendable sheaf codes," Mar. 2024, arXiv:2403.03651v1 [cs.IT].

[39] J. H. C. Whitehead, "Combinatorial homotopy. I," *Bull. (New Ser.) Amer. Math. Soc.*, vol. 55, no. 3, pp. 213–245, Mar. 1949.

[40] D. A. Holton and J. Sheehan, *The Petersen Graph*. Cambridge, U.K.: Cambridge University Press, Apr. 1993.

[41] P.-H. Leemann, "Schreir graphs: Transitivity and coverings," *Int. J. Algebra Comput.*, vol. 26, no. 01, pp. 69–93, Feb. 2016.

[42] M. Morgenstern, "Existence and explicit constructions of $q + 1$ regular Ramanujan graphs for every prime power q," *J. Combinatorial Theory, Ser. B*, vol. 62, no. 1, pp. 44–62, Sep. 1994.

[43] G. Kalachev and P. Panteleev, "Two-sided robustly testable codes," Jun. 2022, arXiv:2206.09973v3 [cs.IT].

[44] A. Leverrier and G. Zémor, private communication, Sep. 2024.

[45] V. Guruswami, A. Rudra, and M. Sudan, *Essential Coding Theory*, 2022. [Online]. Available: https://cse.buffalo.edu/faculty/atri/courses/coding-theory/book/index.html

[46] J. Roffe, D. R. White, S. Burton, and E. Campbell, "Decoding across the quantum low-density parity-check code landscape," *Phys. Rev. Res.*, vol. 2, no. 4, Dec. 2020, Art. no. 043423.

[47] Z. Babar, P. Botsinis, D. Alanis, S. X. Ng, and L. Hanzo, "The road from classical to quantum codes: A hashing bound approaching design procedure," *IEEE Access*, vol. 3, pp. 146–176, 2015.

[48] E. Rosnes and Ø. Ytrehus, "An efficient algorithm to find all small-size stopping sets of low-density parity-check matrices," *IEEE Trans. Inf. Theory*, vol. 55, no. 9, pp. 4167–4178, Sep. 2009.

[49] E. Rosnes, Ø. Ytrehus, M. A. Ambroze, and M. Tomlinson, "Addendum to "An efficient algorithm to find all small-size stopping sets of low-density parity-check matrices"," *IEEE Trans. Inf. Theory*, vol. 58, no. 1, pp. 164–171, Jan. 2012.

Asymptotically Good Generalized Quantum Tanner Codes: Supplementary Material

APPENDIX A
PROOFS

A. Proof of Proposition 2

Since $\mathcal{G}$ acts transitively, given $x, y \in \mathcal{X}$, we can find a $g \in \mathcal{G}$ such that $gx = y$. Therefore, $\mathrm{Aut}_{\mathcal{G}}(\mathcal{X})$ acts freely on $\mathcal{X}$ because given $\sigma \in \mathrm{Aut}_{\mathcal{G}}(\mathcal{X})$ such that $\sigma(x) = x$ for one $x \in \mathcal{X}$, we have

$$\sigma(y) = \sigma(gx) = g\sigma(x) = gx = y.$$

So σ acts trivially on all $y \in \mathcal{X}$, meaning $\sigma = 1 \in \mathrm{Aut}_{\mathcal{G}}(\mathcal{X})$.

Moreover, if $\mathcal{G}$ also acts freely on $\mathcal{X}$, for given $x, y \in \mathcal{X}$ we can define the function $\sigma_{x,y} : \mathcal{X} \to \mathcal{X}$ by

$$\sigma_{x,y}(z) = g_{x,z}y$$

for $z \in \mathcal{X}$, where $g_{x,z} \in \mathcal{G}$ is the unique element mapping x to z, i.e., $g_{x,z}x = z$. Now, observe that for any $h \in \mathcal{G}$ we have

$$h\sigma_{x,y}(z) = hg_{x,z}y \overset{(a)}{=} g_{x,hz}y = \sigma_{x,y}(hz),$$

where (a) holds because $hg_{x,z}x = hz$ and $g_{x,hz}$ is the unique element such that $g_{x,hz}x = hz$. This indicates that $\sigma_{x,y}$ is an element of $\mathrm{Aut}_{\mathcal{G}}(\mathcal{X})$ by definition. We conclude that $\mathrm{Aut}_{\mathcal{G}}(\mathcal{X})$ acts transitively on $\mathcal{X}$ since

$$\sigma_{x,y}(x) = g_{x,x}y = 1y = y,$$

where $1 \in \mathcal{G}$ is the neutral element of the group.

Conversely, we want to show that if $\mathrm{Aut}_{\mathcal{G}}(\mathcal{X})$ acts transitively on $\mathcal{X}$, then given $g \in \mathcal{G}$ and some $x \in \mathcal{X}$ such that $gx = x$, it implies $g = 1$. Consider a $y \in \mathcal{X}$ and let $\sigma_{x,y} \in \mathrm{Aut}_{\mathcal{G}}(\mathcal{X})$ such that $\sigma_{x,y}(x) = y$. We have

$$gy = g\sigma_{x,y}(x) \overset{(b)}{=} \sigma_{x,y}(gx) = \sigma_{x,y}(x) = y,$$

where (b) is due to the definition of $\mathrm{Aut}_{\mathcal{G}}(\mathcal{X})$. Hence, g acts trivially on $\mathcal{X}$. We assume that the group action is faithful, so it follows that $g = 1$, and the action is also free.

B. Proof of Proposition 3

Before proving the proposition, we recall some vocabulary used for a Tanner code $\mathscr{D} = \mathrm{Tan}((\mathcal{V}, \mathcal{E}), \mathscr{C}^{\perp})$. Let a $\mathscr{C}$-generator for $\mathscr{D}$ be a vector of $\mathbb{F}_2^{|\mathcal{E}|}$ which is equal to a codeword of $\mathscr{C}$ on the local view of some vertex v, and zero elsewhere. With this terminology, $\mathscr{D}$ is the space orthogonal to all $\mathscr{C}$-generators.

Without loss of generality, let $\mathcal{A} = \{a_1, \ldots, a_\Delta\}$ and $\mathcal{B} = \{b_1, \ldots, b_\Delta\}$. Next, let $\boldsymbol{v}$ be a $(\mathscr{C}_{\mathrm{A}} \otimes \mathscr{C}_{\mathrm{B}})$-generator for $\mathscr{C}_0$, and let $\boldsymbol{w}$ be a $(\mathscr{C}_{\mathrm{A}}^{\perp} \otimes \mathscr{C}_{\mathrm{B}}^{\perp})$-generator for $\mathscr{C}_1$, supported on $\mathcal{E}_0^{\mathcal{Q}}(v)$ and $\mathcal{E}_1^{\mathcal{Q}}(w)$, respectively. If these supports overlap, then $(v, 0)$ and $(w, 1)$ are connected by either edges in $\mathscr{G}_{\mathrm{A}}$ or edges in $\mathscr{G}_{\mathrm{B}}$. Without loss of generality, suppose the edges are from $\mathscr{G}_{\mathrm{A}}$ and are labeled by $\{a_i : i \in \mathcal{I}\}$ in $\mathcal{E}_{\mathrm{A}}(v, 0)$ and by $\{a_{i'} : i' \in \mathcal{I}'\}$ in $\mathcal{E}_{\mathrm{A}}(w, 1)$, for some subsets $\mathcal{I}, \mathcal{I}' \subseteq [\Delta]$ of the same size. Then the overlap between $\mathcal{E}_0^{\mathcal{Q}}(v)$ and $\mathcal{E}_1^{\mathcal{Q}}(w)$ will be labeled by $\{(a_i, b_j) : i \in \mathcal{I}, j \in [\Delta]\}$ in $\mathcal{E}_0^{\mathcal{Q}}(v)$ and by $\{(a_{i'}, b_j) : i' \in \mathcal{I}', j \in [\Delta]\}$ in $\mathcal{E}_1^{\mathcal{Q}}(w)$. By the definition of the tensor code (see Definition 7), the generator $\boldsymbol{v}$ is now a codeword of $\mathscr{C}_{\mathrm{B}}$ on the set $\{(a_i, b_j) : j \in [\Delta]\}$ for each $i \in \mathcal{I}$, while $\boldsymbol{w}$ is a codeword of $\mathscr{C}_{\mathrm{B}}^{\perp}$ on the set $\{(a_{i'}, b_j) : j \in [\Delta]\}$ for each $i' \in \mathcal{I}'$, so $\boldsymbol{v}$ and $\boldsymbol{w}$ are orthogonal. Recall that the definition of $\boldsymbol{v}$ and $\boldsymbol{w}$ implies that $\mathscr{C}_0^{\perp}$ is the span of all such $\boldsymbol{v}$ and $\mathscr{C}_1$ is the space orthogonal to all such $\boldsymbol{w}$. We conclude that $\mathscr{C}_0^{\perp} \subseteq \mathscr{C}_1$, and hence the codes form a CSS code. For the LDPC part, we can keep the degree Δ of the graphs involved fixed while letting the number of vertices they have grow.

C. Proof of Proposition 7

The adjacency matrix of $\mathscr{G}$ can be written as the sum

$$\left[\begin{array}{c|c} \mathsf{A}_1 & \mathsf{A}_2 \\ \hline \mathsf{A}_2 & \mathsf{A}_3 \end{array}\right] = \left[\begin{array}{c|c} 0 & \mathsf{A}_2 \\ \hline \mathsf{A}_2 & 0 \end{array}\right] + \left[\begin{array}{c|c} \mathsf{A}_1 & 0 \\ \hline 0 & \mathsf{A}_3 \end{array}\right].$$

Recall that the first summand has eigenvalues $\pm$ the eigenvalues of A_2. Let R be an orthogonal matrix diagonalizing it such that Δ and $-\Delta$ are the two first entries on the diagonal matrix, and let D denote the rest of the matrix. Here, Δ is the regularity of the three graphs, and hence also the largest eigenvalue of their adjacency matrices A_1, A_2, and A_3. We get

$$\mathsf{R}\left[\begin{array}{c|c} 0 & \mathsf{A}_2 \\ \hline \mathsf{A}_2 & 0 \end{array}\right]\mathsf{R}^{\mathsf{T}} = \left[\begin{array}{cc|c} \Delta & 0 & 0 \\ 0 & -\Delta & \\ \hline & 0 & \mathsf{D} \end{array}\right].$$

Now since $(\boldsymbol{u}, \boldsymbol{u})$ and $(\boldsymbol{u}, -\boldsymbol{u})$ are eigenvectors corresponding to Δ and $-\Delta$, respectively, in the first matrix, and both correspond to Δ in the second, we have

$$\mathsf{R}\left[\begin{array}{c|c} \mathsf{A}_1 & 0 \\ \hline 0 & \mathsf{A}_3 \end{array}\right]\mathsf{R}^{\mathsf{T}} = \left[\begin{array}{cc|c} \Delta & 0 & 0 \\ 0 & \Delta & \\ \hline & 0 & \mathsf{M} \end{array}\right]$$

for some matrix M with $\max(\lambda(\mathscr{G}_{\mathrm{A}_1}), \lambda(\mathscr{G}_{\mathrm{A}_3}))$ as its largest eigenvalue. To get the zeros in the upper right block, consider an entry w_{ij} there, and let the columns of R be $\boldsymbol{r}_1, \ldots, \boldsymbol{r}_{2m}$, where m is the number of vertices in the original graphs. Furthermore, let $\sum_{t=1}^{2m} \mu_t \boldsymbol{v}_t \boldsymbol{v}_t^{\mathsf{T}}$ be a spectral decomposition of $\mathsf{A}_1 \oplus \mathsf{A}_3$ where $\boldsymbol{v}_1 = \boldsymbol{r}_1$ and $\boldsymbol{v}_2 = \boldsymbol{r}_2$. We get

$$\begin{aligned} w_{ij} = \boldsymbol{r}_i^{\mathsf{T}}(\mathsf{A}_1 \oplus \mathsf{A}_3)\boldsymbol{r}_j &= \boldsymbol{r}_i^{\mathsf{T}}\left(\sum_{t=1}^{2m} \mu_t \boldsymbol{v}_t \boldsymbol{v}_t^{\mathsf{T}}\right)\boldsymbol{r}_j \\ &= \sum_{t=1}^{2m} \mu_t \boldsymbol{r}_i^{\mathsf{T}} \boldsymbol{v}_t \boldsymbol{v}_t^{\mathsf{T}} \boldsymbol{r}_j = \mu_i \boldsymbol{r}_i^{\mathsf{T}} \boldsymbol{v}_i \boldsymbol{v}_i^{\mathsf{T}} \boldsymbol{r}_j = \mu_i \boldsymbol{v}_i^{\mathsf{T}} \boldsymbol{r}_j = 0, \end{aligned}$$

where the two last equalities follow as $i \in [2]$ implies $\boldsymbol{r}_i = \boldsymbol{v}_i$. The lower left block is similar, but with

$$w_{ij} = \mu_j \boldsymbol{r}_i^{\mathsf{T}} \boldsymbol{v}_j \boldsymbol{v}_j^{\mathsf{T}} \boldsymbol{r}_j = \mu_j \boldsymbol{r}_i^{\mathsf{T}} \boldsymbol{v}_j = 0,$$

as $j \in [2]$.

We now have

$$\mathsf{R}\left[\begin{array}{c|c} \mathsf{A}_1 & \mathsf{A}_2 \\ \hline \mathsf{A}_2 & \mathsf{A}_3 \end{array}\right]\mathsf{R}^{\mathsf{T}} = \left[\begin{array}{cc|c} 2\Delta & 0 & \\ 0 & 0 & 0 \\ \hline & 0 & \mathsf{D}+\mathsf{M} \end{array}\right],$$

and the largest eigenvalue of the sum of two symmetric matrices D and M cannot be larger than the sum of their largest eigenvalues. This sum is $\lambda(\mathscr{G}_{\mathrm{A}_2}) + \max(\lambda(\mathscr{G}_{\mathrm{A}_1}), \lambda(\mathscr{G}_{\mathrm{A}_3}))$, so $\lambda(\mathscr{G})$, the second largest eigenvalue of the matrix, cannot be larger than this value.

D. Proof of Lemma 10

We give the proof for $\mathcal{S}_{00}^{\mathrm{e}}$ and note that the other cases are similar. View $\boldsymbol{x}^0 = \boldsymbol{C}_0 + \boldsymbol{R}_0$ as a subgraph of $\mathscr{G}_0^{\square}$. The vertices $\mathcal{S}_{00}^{\mathrm{e}}$ have degree at least $\kappa\Delta\frac{1}{2}\alpha\Delta$ because the code is κ-product-expanding. Note that the minimality of $||\boldsymbol{C}_0||_{\mathrm{C}} + ||\boldsymbol{R}_0||_{\mathrm{R}} + ||\boldsymbol{C}_1||_{\mathrm{C}} + ||\boldsymbol{R}_1||_{\mathrm{R}}$ is needed here. The Expander Mixing Lemma (Lemma 2) for the bipartite graph $\mathscr{G}_0^{\square}$ gives

$$\begin{aligned} |\mathcal{S}_{00}^{\mathrm{e}}|\frac{1}{2}\alpha\kappa\Delta^2 &\le |\mathcal{E}(\mathcal{S}_{00}^{\mathrm{e}}, \mathcal{S}_{11})| \\ &\le \Delta^2 \frac{|\mathcal{S}_{00}^{\mathrm{e}}||\mathcal{S}_{11}|}{|\mathcal{V}_{00}|} + 8\Delta\sqrt{|\mathcal{S}_{00}^{\mathrm{e}}||\mathcal{S}_{11}|}. \end{aligned}$$

Using the hypothesis of the lemma, $|\mathcal{S}_{ij}| \le \frac{1}{2}\frac{\alpha\kappa}{2}|\mathcal{V}_{00}|$, we get

$$\begin{aligned} |\mathcal{S}_{00}^{\mathrm{e}}|\frac{1}{2}\alpha\kappa\Delta^2 &\le \frac{1}{2}|\mathcal{S}_{00}^{\mathrm{e}}|\frac{1}{2}\alpha\kappa\Delta^2 + 8\Delta\sqrt{|\mathcal{S}_{00}^{\mathrm{e}}||\mathcal{S}_{11}|}, \\ \frac{1}{2}\sqrt{|\mathcal{S}_{00}^{\mathrm{e}}|}\frac{1}{2}\alpha\kappa\Delta^2 &\le 8\Delta\sqrt{|\mathcal{S}_{11}|}, \\ |\mathcal{S}_{00}^{\mathrm{e}}| &\le \frac{256}{(\frac{1}{2}\alpha)^2\kappa^2\Delta^2}|\mathcal{S}_{11}| \le \frac{256}{(\frac{1}{2}\alpha)^2\kappa^2\Delta^2}|\mathcal{S}_0|. \end{aligned}$$

E. Proof of Lemma 11

We only treat the case $i = j = 0$. The proof is similar in the other cases. If we only keep the vertices $\mathcal{V}_{00}$ and $\mathcal{V}_{01}$, we obtain a graph by treating the squares as edges. By treating squares that belong to the same column in some local view $\mathcal{E}^{\square}(v)$ for $v \in \mathcal{V}_{00} \cup \mathcal{V}_{01}$ as equal, we recover the double cover of $\mathscr{G}_{\mathrm{A}}$. The codeword $\boldsymbol{x}$ induces a subgraph consisting of the edges corresponding to nonzero rows in $\boldsymbol{x}$.

In this subgraph, every vertex in $\mathcal{T}$ has degree at least the minimum weight of a codeword in $\mathscr{C}_{\mathrm{A}}$ minus the amount of nonzero coordinates it has in common with $\boldsymbol{R}_i$. If $v \in \mathcal{V}_{ij}$ is ordinary, $||\boldsymbol{c}_v||_{\mathrm{c}} + ||\boldsymbol{r}_v||_{\mathrm{r}} < \frac{1}{2}\alpha\Delta$ by definition, so any column of $\boldsymbol{c}_v$ must clearly have less than $\frac{1}{2}\alpha\Delta$ overlapping nonzero indices with rows of $\boldsymbol{r}_v$. This means vertices in $\mathcal{T}$ has at least weight $\delta\Delta - \frac{1}{2}\alpha\Delta$, which we can bound by the more readable $\frac{1}{2}\delta\Delta$. These edges are going to $\mathcal{S}_{01}$, so we get

$$|\mathcal{T}|\frac{1}{2}\delta\Delta \le |\mathcal{E}(\mathcal{S}_{01}, \mathcal{T})|.$$

If we had been considering the other definition of $\mathcal{T}$, we would now be looking at $\mathscr{G}_{\mathrm{B}}$ instead of $\mathscr{G}_{\mathrm{A}}$, and we would be looking at a graph with two components instead of a connected one. In that case $|\mathcal{E}(\mathcal{S}_{01}, \mathcal{T})|$ will be largest when $\mathcal{S}_{01}$ and $\mathcal{T}$ both fall in the same component. The Expander Mixing Lemma for the double cover of such a component gives

$$|\mathcal{E}(\mathcal{S}_{01}, \mathcal{T})| \le \Delta\frac{|\mathcal{S}_{01}||\mathcal{T}|}{\frac{1}{2}|\mathcal{V}_{01}|} + 2\sqrt{2}\sqrt{\Delta}\sqrt{|\mathcal{S}_{01}||\mathcal{T}|}.$$

Using the hypothesis $|\mathcal{S}_{ij}| \le \delta|\mathcal{V}_{00}|/8$ and combining the inequalities, we get

$$\begin{aligned} |\mathcal{T}|\frac{1}{2}\delta\Delta &\le \Delta\frac{\delta}{4}|\mathcal{T}| + 2\sqrt{2}\sqrt{\Delta}\sqrt{|\mathcal{S}_{01}||\mathcal{T}|}, \\ \Delta|\mathcal{T}|\left(\frac{\delta}{4}\right)^2 &\le 8|\mathcal{S}_{01}| \end{aligned}$$

and the claim follows.

F. Proof of Lemma 12

Let $\boldsymbol{x} \in \mathscr{C}_1 \setminus \mathscr{C}_0^{\perp}$ be given, and assume

$$||\boldsymbol{x}|| < \frac{1}{2}\frac{\delta^2\kappa n}{512\Delta^2}.$$

Without loss of generality, we may assume that the minimal value of $||\boldsymbol{x}||$ is achieved inside the coset $\boldsymbol{x} + \mathscr{C}_0^{\perp}$, and that $(\boldsymbol{C}_0, \boldsymbol{R}_0, \boldsymbol{C}_1, \boldsymbol{R}_1)$ is a minimal representation for $\boldsymbol{x}$. Note that

$$\begin{aligned} |\mathcal{S}_{ij}| &\le ||\boldsymbol{C}_j||_{\mathrm{C}} + ||\boldsymbol{R}_i||_{\mathrm{R}} \\ &\le ||\boldsymbol{C}_0||_{\mathrm{C}} + ||\boldsymbol{R}_0||_{\mathrm{R}} + ||\boldsymbol{C}_1||_{\mathrm{C}} + ||\boldsymbol{R}_1||_{\mathrm{R}} = ||\boldsymbol{x}|| \end{aligned}$$

implies that

$$|\mathcal{S}_{ij}| < \frac{1}{2}\frac{\delta^2\kappa n}{512\Delta^2} = \frac{1}{2}\frac{\alpha\kappa}{2}|\mathcal{V}_{00}|,$$

so that Lemma 10 holds. Lemma 11 holds as well, as

$$\frac{1}{2}\frac{\alpha\kappa}{2} = \frac{1}{2}\frac{\delta^2}{512}\kappa < \delta/8,$$

where the last inequality holds as $\delta \le 1$ and $\kappa < 3/2$ [KP22, Sec. 3].[9]

Suppose, without loss of generality, that $|\mathcal{S}_1| \ge |\mathcal{S}_0|$ and $|\mathcal{S}_{10}| \ge |\mathcal{S}_{01}|$. For any constant $\frac{1}{2} < \gamma < 1$, the number of ordinary vertices of $\mathcal{S}_{10}$ will be larger than $\gamma|\mathcal{S}_{10}|$ for Δ large enough by Lemma 10.

Suppose, without loss of generality, that the number of ordinary columns in the local views of vertices of $\mathcal{S}_{10}$ is at least $\frac{\gamma}{2}|\mathcal{S}_{10}|$. Lemma 11 tells us that these ordinary columns are columns in local views of the vertices of $\mathcal{T}$ of size bounded above by $\frac{2\cdot 64}{\delta^2\Delta}|\mathcal{S}_{01}| \le \frac{2\cdot 64}{\delta^2\Delta}|\mathcal{S}_{10}|$. This means that the average number of nonzero columns of $\boldsymbol{C}_0$ on the local views of vertices of $\mathcal{T}$ is at least $\frac{\gamma}{2}|\mathcal{S}_{10}|/(\frac{2\cdot 64}{\delta^2\Delta}|\mathcal{S}_{10}|) = \gamma\frac{\delta^2\Delta}{2\cdot 128} = \gamma\alpha\Delta$. Recall that the required amount for being exceptional is $\frac{1}{2}\alpha\Delta$, so a constant proportion of the vertices $\mathcal{T} \subseteq \mathcal{S}_{00}$ must be exceptional for any fixed Δ. The maximal amount of columns that can fit in the local view of a vertex is Δ, so

$$|\mathcal{T}| \ge \left(\frac{\gamma}{2}|\mathcal{S}_{10}|\right)/\Delta \ge \frac{\gamma}{4\Delta}|\mathcal{S}_1| \ge \frac{\gamma}{4\Delta}|\mathcal{S}_0|.$$

However, Lemma 10 limits the number of exceptional vertices of $\mathcal{S}_{00}$ to $O(1/\Delta^2)|\mathcal{S}_0|$, which "a constant proportion of" $\frac{\gamma}{4\Delta}|\mathcal{S}_0|$ will exceed for large enough Δ.

[9]The product-expansion κ for a pair of codes of rates $\epsilon_1 - 1$, $\epsilon_2 - 1$ is bounded above by $\epsilon_1\epsilon_2 + 1/2$. This is analogous to the Singleton bound for the minimum distance of a code.

G. Proof of Theorem 3

Let a codeword $\boldsymbol{x} \in \mathscr{C}_1 \setminus \mathscr{C}_0^\perp$ with minimal representation $(\boldsymbol{C}_0, \boldsymbol{R}_0, \boldsymbol{C}_1, \boldsymbol{R}_1)$ be given. This means that

$$\boldsymbol{x} = \boldsymbol{C}_1 + \boldsymbol{R}_0 = \sum_{v \in \mathcal{V}_{01}} (\boldsymbol{c}_v + \boldsymbol{r}_v).$$

Since the local code is κ-product-expanding and the representation of $\boldsymbol{x}$ is minimal, we have

$$|\boldsymbol{x}| = \sum_{v \in \mathcal{V}_{01}} |\boldsymbol{c}_v + \boldsymbol{r}_v| \geq \sum_{v \in \mathcal{V}_{01}} \kappa\Delta(||\boldsymbol{c}_v||_{\mathrm{c}} + ||\boldsymbol{r}_v||_{\mathrm{r}}),$$

meaning $|\boldsymbol{x}| \geq \kappa\Delta(||\boldsymbol{C}_1||_{\mathrm{C}} + ||\boldsymbol{R}_0||_{\mathrm{R}})$. The same argument can be applied when writing $\boldsymbol{x} = \boldsymbol{C}_0 + \boldsymbol{R}_1$, yielding $|\boldsymbol{x}| \geq \kappa\Delta(||\boldsymbol{C}_0||_{\mathrm{C}} + ||\boldsymbol{R}_1||_{\mathrm{R}})$. Combining these, we get

$$|\boldsymbol{x}| \geq \kappa\Delta\frac{1}{2}(||\boldsymbol{C}_1||_{\mathrm{C}} + ||\boldsymbol{R}_0||_{\mathrm{R}} + ||\boldsymbol{C}_0||_{\mathrm{C}} + ||\boldsymbol{R}_1||_{\mathrm{R}}) = \kappa\Delta\frac{1}{2}||\boldsymbol{x}||,$$

and the result follows from Lemma 12 by the symmetry of $\mathscr{C}_0$ and $\mathscr{C}_1$.

Appendix B
Parity-Check Matrix Construction

We give a short description of how parity-check matrices for $\mathscr{C}_0 = \mathrm{Tan}(\mathscr{G}_0^\square, (\mathscr{C}_\mathrm{A} \otimes \mathscr{C}_\mathrm{B})^\perp)$ and $\mathscr{C}_1 = \mathrm{Tan}(\mathscr{G}_1^\square, (\mathscr{C}_\mathrm{A}^\perp \otimes \mathscr{C}_\mathrm{B}^\perp)^\perp)$ from Definition 10 may be constructed.

We assume an ordering on the edges of $\mathscr{G}_i^\square = (\mathcal{V}_i, \mathcal{E}_i^\mathcal{Q})$ such that $e_0 \in \mathcal{E}_0^\mathcal{Q}$ and $e_1 \in \mathcal{E}_1^\mathcal{Q}$ appear at the same place of the two ordered sets when they come from the same square of the complex $\mathcal{X}$, making the sets of edges $\mathcal{E}_i^\mathcal{Q} = \{e_{i,1}, \ldots, e_{i,n}\}$. Here, n is the length of the code, which is equal to $|\mathcal{E}_i^\mathcal{Q}| = |\mathcal{V}_0|\Delta^2/2$. We also order the vertices $\mathcal{V}_i = \{v_{i,1}, \ldots, v_{i,|\mathcal{V}_0|}\}$ and write $\mathcal{A} = \{a_1, \ldots, a_\Delta\}$ and $\mathcal{B} = \{b_1, \ldots, b_\Delta\}$.

For an $m_\mathrm{A} \times n_\mathrm{A}$ matrix A and an $m_\mathrm{B} \times n_\mathrm{B}$ matrix B, their *Kronecker product* is the $m_\mathrm{A}m_\mathrm{B} \times n_\mathrm{A}n_\mathrm{B}$ matrix

$$\mathsf{A} \otimes \mathsf{B} = \begin{bmatrix} a_{11}\mathsf{B} & \ldots & a_{1n_\mathrm{A}}\mathsf{B} \\ \vdots & \ddots & \vdots \\ a_{m_\mathrm{A}1}\mathsf{B} & \ldots & a_{m_\mathrm{A}n_\mathrm{A}}\mathsf{B} \end{bmatrix}.$$

The codewords of the tensor code from Definition 7 are defined as $n_\mathrm{A} \times n_\mathrm{B}$ matrices C. When we flatten them into vectors of length $n_\mathrm{A}n_\mathrm{B}$ by stacking the rows of the matrices, we get codewords of the form

$$\boldsymbol{c} = (c_{11}, \ldots, c_{1n_\mathrm{B}}, \ldots, c_{n_\mathrm{A}1}, \ldots, c_{n_\mathrm{A}n_\mathrm{B}}).$$

It is clear that the Kronecker product $\mathsf{H}_\mathrm{A} \otimes \mathsf{H}_\mathrm{B}$ becomes a parity-check matrix for the flattened version of

$$(\mathscr{C}_\mathrm{A}^\perp \otimes \mathscr{C}_\mathrm{B}^\perp)^\perp = \mathscr{C}_\mathrm{A} \otimes \mathbb{F}_2^{n_\mathrm{B}} + \mathbb{F}_2^{n_\mathrm{A}} \otimes \mathscr{C}_\mathrm{B}$$

if H_A and H_B are parity-check matrices for $\mathscr{C}_\mathrm{A}$ and $\mathscr{C}_\mathrm{B}$, respectively.

To see this, recall that given vectors $\boldsymbol{u} = (u_1, \ldots, u_{n_\mathrm{A}}) \in \mathbb{F}_2^{n_\mathrm{A}}$ and $\boldsymbol{v} = (v_1, \ldots, v_{n_\mathrm{B}}) \in \mathbb{F}_2^{n_\mathrm{B}}$, we have

$$\boldsymbol{u} \otimes \boldsymbol{v} = (u_1v_1, \ldots, u_1v_{n_\mathrm{B}}, \ldots, u_{n_\mathrm{A}}v_1, \ldots, u_{n_\mathrm{A}}v_{n_\mathrm{B}}).$$

A flattened codeword $\boldsymbol{c}$ of $\mathscr{C}_\mathrm{A} \otimes \mathbb{F}_2^{n_\mathrm{B}} + \mathbb{F}_2^{n_\mathrm{A}} \otimes \mathscr{C}_\mathrm{B}$ can be written on the form

$$\boldsymbol{c} = \sum_{j=1}^{n_\mathrm{B}} \boldsymbol{c}_{\mathrm{A}j} \otimes \boldsymbol{e}_j + \sum_{i=1}^{n_\mathrm{A}} \boldsymbol{e}_i \otimes \boldsymbol{c}_{\mathrm{B}i},$$

where $\boldsymbol{c}_{\mathrm{A}j} \in \mathscr{C}_\mathrm{A}$, $\boldsymbol{c}_{\mathrm{B}i} \in \mathscr{C}_\mathrm{B}$, and $\boldsymbol{e}_i = (0, \ldots 0, 1, 0, \ldots, 0)$ with 1 in the i-th position. Now $\boldsymbol{c}$ is in the nullspace of $\mathsf{H}_\mathrm{A} \otimes \mathsf{H}_\mathrm{B}$ since

$$\begin{aligned}(\mathsf{H}_\mathrm{A} \otimes \mathsf{H}_\mathrm{B})\boldsymbol{c}^\mathsf{T} &= \sum_{j=1}^{n_\mathrm{B}} \mathsf{H}_\mathrm{A}\boldsymbol{c}_{\mathrm{A}j}^\mathsf{T} \otimes \mathsf{H}_\mathrm{B}\boldsymbol{e}_j^\mathsf{T} + \sum_{i=1}^{n_\mathrm{A}} \mathsf{H}_\mathrm{A}\boldsymbol{e}_i^\mathsf{T} \otimes \mathsf{H}_\mathrm{B}\boldsymbol{c}_{\mathrm{B}i}^\mathsf{T} \\ &= \sum_{j=1}^{n_\mathrm{B}} \boldsymbol{0}^\mathsf{T} \otimes \mathsf{H}_\mathrm{B}\boldsymbol{e}_j^\mathsf{T} + \sum_{i=1}^{n_\mathrm{A}} \mathsf{H}_\mathrm{A}\boldsymbol{e}_i^\mathsf{T} \otimes \boldsymbol{0}^\mathsf{T} = \boldsymbol{0}^\mathsf{T}.\end{aligned}$$

It is well-known that

$$\mathrm{rank}(\mathsf{H}_\mathrm{A} \otimes \mathsf{H}_\mathrm{B}) = \mathrm{rank}(\mathsf{H}_\mathrm{A})\mathrm{rank}(\mathsf{H}_\mathrm{B}),$$

implying that $\mathscr{C}_\mathrm{A} \otimes \mathbb{F}_2^{n_\mathrm{B}} + \mathbb{F}_2^{n_\mathrm{A}} \otimes \mathscr{C}_\mathrm{B}$, flattened, is equal to the nullspace of $\mathsf{H}_\mathrm{A} \otimes \mathsf{H}_\mathrm{B}$ since the dimension of a tensor code $\mathscr{C}_\mathrm{A} \otimes \mathscr{C}_\mathrm{B}$ is the product of the dimensions of $\mathscr{C}_\mathrm{A}$ and $\mathscr{C}_\mathrm{B}$.

Similarly, let $\mathsf{H}_\mathrm{A}^\perp$ and $\mathsf{H}_\mathrm{B}^\perp$ denote parity-check matrices for $\mathscr{C}_\mathrm{A}^\perp$ and $\mathscr{C}_\mathrm{B}^\perp$, respectively, so that $\mathsf{H}_\mathrm{A}^\perp \otimes \mathsf{H}_\mathrm{B}^\perp$ is a parity-check matrix for the flattened version of $(\mathscr{C}_\mathrm{A} \otimes \mathscr{C}_\mathrm{B})^\perp$. However, in the following subsection, we give an alternative construction for parity-check matrices for $(\mathscr{C}_\mathrm{A} \otimes \mathscr{C}_\mathrm{B})^\perp$ and $(\mathscr{C}_\mathrm{A}^\perp \otimes \mathscr{C}_\mathrm{B}^\perp)^\perp$.

To make the local views of $\mathscr{G}_i^\square$ fit the above convention, we order them as

$$\mathcal{E}_i^\mathcal{Q}(v_{i,j}) = \{e_{i,j_1}, \ldots, e_{i,j_{\Delta^2}}\}$$

for $i \in \{0, 1\}$ and $j \in [|\mathcal{V}_0|]$ so that their labels are

$$\{(a_1, b_1), \ldots, (a_1, b_\Delta), \ldots, (a_\Delta, b_1), \ldots, (a_\Delta, b_\Delta)\}.$$

We construct a parity-check matrix H_0 for $\mathscr{C}_0$ in the following way. Start with a $0 \times |\mathcal{E}_0^\mathcal{Q}|$ matrix H_0 of height 0 and width $|\mathcal{E}_0^\mathcal{Q}|$. For each vertex $v_{0,j} \in \mathcal{V}_0$, concatenate to H_0 from below the 0-matrix of the same height, $k_\mathrm{A}k_\mathrm{B}$, as $\mathsf{H}_\mathrm{A}^\perp \otimes \mathsf{H}_\mathrm{B}^\perp$ (which is the parity-check matrix for $(\mathscr{C}_\mathrm{A} \otimes \mathscr{C}_\mathrm{B})^\perp$, but flattened) and the same width as H_0. Then, distribute the columns of $\mathsf{H}_\mathrm{A}^\perp \otimes \mathsf{H}_\mathrm{B}^\perp$ over the columns of this newly concatenated block so that column m in the block is column l in $\mathsf{H}_\mathrm{A}^\perp \otimes \mathsf{H}_\mathrm{B}^\perp$ when the m-th edge of $\mathscr{G}_0^\square$ is the l-th edge of $\mathcal{E}_0^\mathcal{Q}(v_{0,j})$ (which in symbols is $e_{0,m} = e_{0,j_l}$), $l \in [\Delta^2]$. The resulting matrix is sketched below.

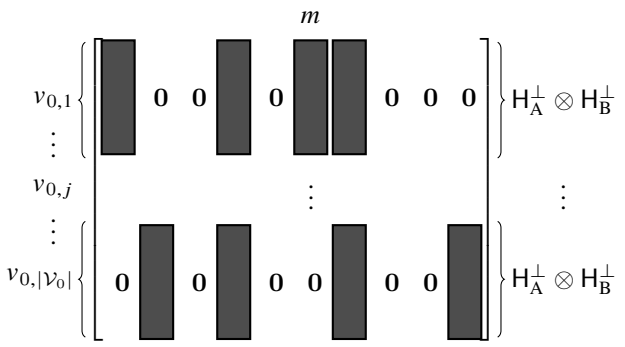

For $\mathscr{C}_1$, we can construct a parity-check matrix in the same way, just swapping the graph $\mathscr{G}_0^\square$ for $\mathscr{G}_1^\square$ and the matrix $\mathsf{H}_\mathrm{A}^\perp \otimes \mathsf{H}_\mathrm{B}^\perp$ for $\mathsf{H}_\mathrm{A} \otimes \mathsf{H}_\mathrm{B}$. Note that the height of $\mathsf{H}_\mathrm{A} \otimes \mathsf{H}_\mathrm{B}$ is $(n - k_\mathrm{A})(n - k_\mathrm{B})$.

More concretely, we can construct the $|\mathcal{V}_0|k_\mathrm{A}k_\mathrm{B} \times n$ parity-check matrix H_0 for $\mathscr{C}_0$ described above as

$$(\mathsf{H}_0)_{st} = \begin{cases} 0 & \text{if } e_{0,t} \notin \mathcal{E}_0^{\mathcal{Q}}(v_{0,j}) \\ (\mathsf{H}_\mathrm{A}^\perp \otimes \mathsf{H}_\mathrm{B}^\perp)_{rl} & \text{if } e_{0,t} = e_{0,j_l} \in \mathcal{E}_0^{\mathcal{Q}}(v_{0,j}), \\ & \text{for some } l \in [\Delta^2], \end{cases}$$

where

$$j = \lceil s/(k_\mathrm{A}k_\mathrm{B}) \rceil,$$
$$r = ((s-1) \mod k_\mathrm{A}k_\mathrm{B}) + 1,$$

for $s \in [|\mathcal{V}_0|k_\mathrm{A}k_\mathrm{B}]$ and $t \in [n]$. Here, $(\cdot)_{st}$ denotes the entry in row s and column t of its matrix argument. Similarly, the $|\mathcal{V}_0|(n-k_\mathrm{A})(n-k_\mathrm{B}) \times n$ parity-check matrix H_1 for $\mathscr{C}_1$ can be given as

$$(\mathsf{H}_1)_{st} = \begin{cases} 0 & \text{if } e_{1,t} \notin \mathcal{E}_1^{\mathcal{Q}}(v_{1,j}) \\ (\mathsf{H}_\mathrm{A} \otimes \mathsf{H}_\mathrm{B})_{rl} & \text{if } e_{1,t} = e_{1,j_l} \in \mathcal{E}_1^{\mathcal{Q}}(v_{1,j}), \\ & \text{for some } l \in [\Delta^2], \end{cases}$$

where

$$j = \lceil s/((n_\mathrm{A}-k_\mathrm{A})(n_\mathrm{B}-k_\mathrm{B})) \rceil,$$
$$r = ((s-1) \mod (n_\mathrm{A}-k_\mathrm{A})(n_\mathrm{B}-k_\mathrm{B})) + 1,$$

for $s \in [|\mathcal{V}_0|(n-k_\mathrm{A})(n-k_\mathrm{B})]$ and $t \in [n]$.

A. Alternative Parity-Check Matrix Construction for the Dual Tensor Code $(\mathscr{C}_\mathrm{A} \otimes \mathscr{C}_\mathrm{B})^\perp$

Here, we give an alternative construction for a parity-check matrix for a tensor product code. By taking the dual, this gives parity-check matrices for $(\mathscr{C}_\mathrm{A} \otimes \mathscr{C}_\mathrm{B})^\perp$ and $(\mathscr{C}_\mathrm{A}^\perp \otimes \mathscr{C}_\mathrm{B}^\perp)^\perp$ that can be used instead of $\mathsf{H}_\mathrm{A}^\perp \otimes \mathsf{H}_\mathrm{B}^\perp$ and $\mathsf{H}_\mathrm{A} \otimes \mathsf{H}_\mathrm{B}$ in the construction described above. We used this alternative construction for the codes considered in this work.

The tensor product of two linear codes can be considered as a Tanner code on the complete bipartite graph, where one code is placed on the first half of vertices, and the other code on the rest, as explained in [Tan81], making a construction similar to the one above possible.

As an example, consider $\Delta = 3$ and the complete bipartite graph $\mathcal{K}_{3,3}$, depicted below, with a certain labeling on the local views. From this, the general case should be clear. Each edge has two labels, one in the local view of each endpoint. Here, the two labels are written directly to the right of the edge and show the label of the edge in the local view of the closest vertex. Note that this labeling is not symmetric, so the figure cannot be simplified as in Example 1. Putting bits on the edges and constraints of $\mathscr{C}_\mathrm{A}$ on the white nodes and $\mathscr{C}_\mathrm{B}$ on the gray nodes defines $\mathscr{C}_\mathrm{A} \otimes \mathscr{C}_\mathrm{B}$ if we organize the edges in a 3×3 matrix where the local views of white nodes are columns and the local views of gray nodes are rows.

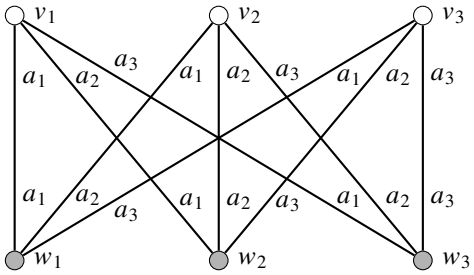

We order the edges lexicographically, so that (v_i, w_j) is edge number $(i-1)\Delta + j$. To build the parity-check matrix, we start by adding the constraints of $\mathscr{C}_\mathrm{B}$ to edges numbered $i\Delta + 1$ to $(i+1)\Delta$ for $i = 0, \ldots, \Delta - 1$, and then add the constraints of $\mathscr{C}_\mathrm{A}$ to the edges $i, \Delta + i, \ldots, \Delta(\Delta-1) + i$ for $i = 1, \ldots, \Delta$. The dual of the resulting matrix was used in place of the Kronecker product when constructing H_0 and H_1 in this paper.

When constructing the dual of a matrix A, we have used the following standard algorithm. First, reduce the matrix to row echelon form in the following way. If the first column of A is nonzero, let i be the smallest i such that $\mathsf{A}_{i1} = 1$, and swap the i-th row of A with the first. Then add the first row of A to all rows where the first element is nonzero. Continue in this way with the matrix where the first row and column of A is removed. Then put the matrix on reduced row echelon form in the following way. Starting with the last row, let j be the position of its first nonzero element. Add the row to all other rows whose j-th element is nonzero. Continue in this way with the second-to-last row and so on. Finally, solve the homogeneous system defined by the resulting matrix.

REFERENCES

[KP22] G. Kalachev and P. Panteleev, "Two-sided robustly testable codes," Jun. 2022, arXiv:2206.09973v3 [cs.IT].

[Tan81] R. M. Tanner, "A recursive approach to low complexity codes," *IEEE Trans. Inf. Theory*, vol. 27, no. 5, pp. 533–547, Sep. 1981.